Deltares

Enabling Delta Life

Effect of the 2017/2018 storm season on the Northwest coast of Ameland

Quick Reaction Force

Deltares

Effect of the 2017/2018 storm season on the Northwest coast of Ameland

Quick Reaction Force

Dennis Korevaar

11202189-002

Deltares

Title
Effect of the 2017/2018 storm season on the Northwest coast of Ameland

Client	Project	Attribute	Pages
Rijkswaterstaat Water, Verkeer en Leefomgeving, UTRECHT	11202189-002	11202189-002-ZWS-0015	60

Keywords
Quick Reaction Force, dune erosion, measurements, XBeach, Ameland Northwest

Summary
The Quick Reaction Force (QRF) was initiated to develop knowledge about the effect of storms on the coast. For this purpose Ameland Northwest was chosen as study site. The foreshore, beach and dunes at Ameland Northwest are a part of a highly dynamic environment. Over the last tens of years considerable erosion occurred at the beach of Ameland Northwest and caused a retreat of hundreds of meters.

This report describes the effect of storm season 2017/2018 on waves and morphology at Ameland Northwest. Over the past decades the beach of Ameland Northwest shows an eroding trend. The QRF performed wave measurements with pressure sensors on the beach during the entire storm season. LiDAR bed level measurements were made before and after the storm season. These measurements were used to validate a 1D-XBeach simulation of beach and dune behaviour. The 2017/2018 storm season was relatively strong. Ten storm surges occurred during which the offshore wave heights were higher than 3 m.

The 1D-XBeach morphodynamics showed good agreement with observed bed level changes in the upper part of the beach profile and the seaward side of the dune. The model was not able to model the erosion of the foreshore. This is likely caused by 2D effects not captured in the 1D model. Three out of the ten storms caused dune erosion, but this only occurred because previous storms eroded the beach.

We recommend using a 2D-XBeach model for Ameland NW and focussing more on one storm instead of the entire storm season. This also requires morphological data on shorter time scales (days). We recommend selecting additional QRF sites along the Dutch coast with more alongshore uniform bathymetry to set-up and validate the 1D-XBeach model approach with. In addition to this, we would recommend having a model of the study area ready before the storm season in order to be able to quickly assess the effects of storms.

We recommend linking up QRF more with long-term projects so that 'fast follow-up studies' have a broader basis and can therefore actually be implemented 'quickly'.

Version	Date	Author	Initials	Review	Initials	Approval	Initials
0.0	Jul. 2018	Dennis Korevaar		Bart Grasmeijer		Dirk-Jan Walstra	
0.1	Aug. 2018	Dennis Korevaar		Bart Grasmeijer		Dirk-Jan Walstra	
1.0	Nov. 2018	Dennis Korevaar		Bart Grasmeijer		Dirk-Jan Walstra	

Status
final

This document is an internship report for the master program ‘Earth, Surface and Water’ at Utrecht University.

Student: Dennis Korevaar
Student number: 4151992

Host organizations: Deltares and Rijkswaterstaat
University: Utrecht University (UU)

Supervisors
Supervisor Deltares: Dr. Ir. Bart Grasmeijer
Supervisor Rijkswaterstaat: Rena Hoogland
Supervisor UU: Prof. Dr. Gerben Ruessink

Date: 31-08-2018

Universiteit Utrecht

Rijkswaterstaat
Ministerie van Infrastructuur en Waterstaat

Deltares
Enabling Delta Life

Contents

1 Introduction

1.1 Quick Reaction Force

In 2014, the Delta Program Wadden Sea Region recommended setting up a Quick Reaction Force (QRF) in which several parties cooperate in the collection, sharing and disclosure of physical data during extreme natural events (IMARES, 2014). The aim is to gain the best possible knowledge before, during and after storms to be able to answer coastal management questions and addressing knowledge gaps in the field of flood risk management.

The need was expressed by various coastal administrators (Rijkswaterstaat, and water boards Noorderzijlvest and Hollands Noorderkwartier) to be able to make an analysis quickly after a storm about the effect on the state of their management area. Administrators need an adequate provision of information (which sometimes has to come from different parties) after a storm, and want insight into whether the actual effects are in line with expectations (on the one hand based on experience of the administrator and on the other hand on the basis of the available models).

Apart from the fact that additional monitoring may be necessary to assess acute risks (e.g. dike watch by the water boards), it also provides more insight into the functioning of the morphodynamic system under extreme conditions for example. There is a need for validation of knowledge about water safety for testing, design and maintenance of flood defences and a need for adequate information about the impact of a storm in the context of national information needs and information provision.

Over the years a lot of knowledge has been developed about the effects of storms on the coast. This knowledge is being applied when assessing the coast as flood defence. However, most of this knowledge comes from laboratory tests. Very limited validation material based on field measurements is available.

Aim of the QRF is to improve water safety knowledge through improved acquisition, access and use of field data around storms. To this aim, the QRF offers a structure for coordination between stakeholders involved in disclosure of field data, acquisition of (possibly extra) measurements and drawing up of joint reports, to promote the cooperation between parties. The ultimate goal is to enhance water safety knowledge.

The QRF defined three research themes:

1. Behaviour coastal fundament and shoal-channel interactions;
2. Dynamics beach, dunes, marsh and overwash areas;
3. Predictability high-water Delfzijl.

Within each research theme, one or more measurement locations have been selected.
In this study the focus will be on the second research theme. The measurement location chosen to study this research theme is Ameland Northwest. Management and knowledge questions have been defined in the framework of the QRF activities.

The relevant QRF management questions are the following:

- What is the role of storms in the mid-term morphological development of Ameland NW?
- What is the reliability of predictions of the morphological developments of Ameland NW during storms and how does that influence the reliability of predictions on the mid-term?

The corresponding QRF knowledge questions are the following:

- What is the morphological development of the foreshore, the beach and the dunes at Ameland Northwest because of storms relative to regular conditions (management question 1)?
- Which hydrodynamic cross- and alongshore processes cause alongshore variation in dune erosion at Ameland Northwest during storms (management question 1, 2)?
- Under which conditions and where do dunes erode so that the dune valley submerges? How does the breach in the dunes develop during the storm (management question 1, 2)?
- What are the consequences of the submergence of the dune valley on the inner dune row? How much of the dune valley is submerged, how does the area develop during and after the storm, and how much erosion takes place at the inner dune row (management question 1)?
- How well are current models able to predict the behaviour of the foreshore, the beach and the dune row at Ameland Northwest during storms (management question 2)?

To effectively measure the morphological changes, it was advised to turn the QRF into action when the expected water levels exceed NAP +2.28 m at measuring station Wierumergronden, or the significant wave height exceeds 5.61 m at measuring station Schiermonnikoog Noord (Deltares, 2017). These thresholds are based on a recurrence interval of one year. The measured water levels and wave heights during the storm season 2017/2018 are shown in Figure 1.1. It should be noted that these are the measured data and the activation of the QRF is based on the predictions. However, these differences were probably small. The available data shows that the QRF-action-threshold was exceeded around 29 October 2017. For practical reasons, it was decided to make wave measurements on the beach not only during a single storm but during the entire storm period and to make LiDAR bed level measurements before and after the storm season.

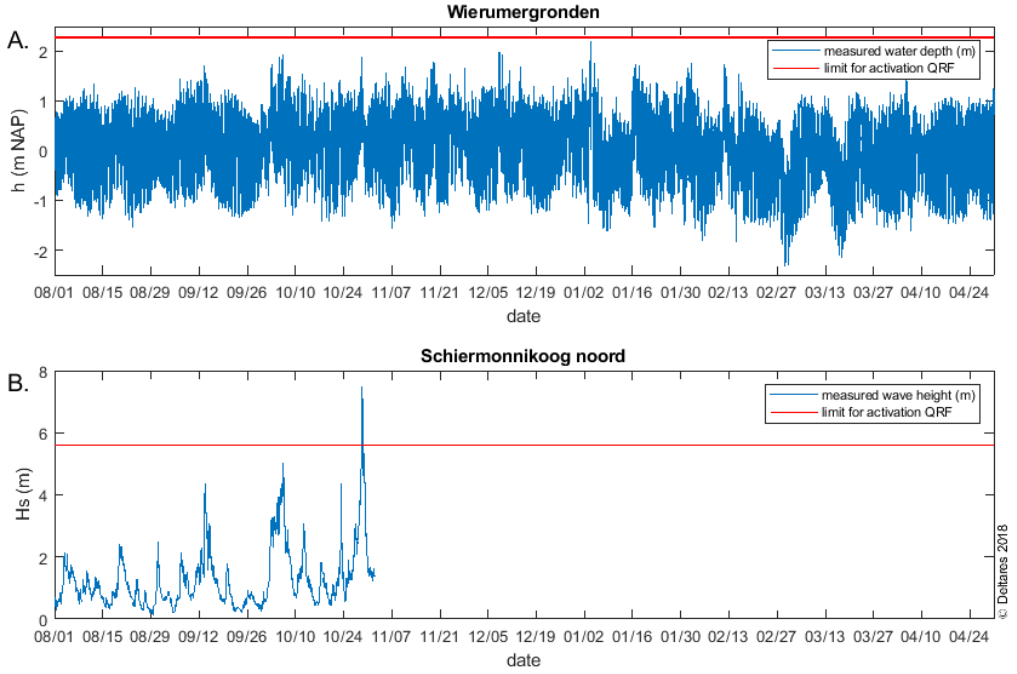

Figure 1.1. A) The measured water levels (m) at measuring station Wierumergronden during the storm season of 2017/2018. B) The measured significant wave height (m) at measuring station Schiermonnikoog Noord during the storm season of 2017/2018. The red line indicates the QRF threshold.

1.2 Ameland Northwest

1.2.1 Site selection

Deltares (2017) describes the background to the QRF location choice. Argument is firstly that the management questions and knowledge questions should have a strong relation with the measurement location. Secondly, at this measurement location the QRF should have the potential to be decisive in answering these questions. Lastly, the measurements should be logistically achievable and existing data and measuring grids which contribute to the results of the QRF should already be available. Based on these criteria Ameland Northwest was chosen. This measurement location covers the QRF theme 'Dynamics beach, dunes, marsh and overwash areas'.

1.2.2 Site description

The study area is shown in Figure 1.2. Ameland Northwest is characterized by two dune rows. The outer dune row is not used as a flood defence and currently shows an eroding trend. On 18 January 2018 even a dune breached occurred near beach pole 3. The second dune row which is located more landward is the primary flood defence. This dune row is partly natural but also partly consists of sand-drift dikes. The height of these dunes is highly variable alongshore. The adjacent dune crests are at least around NAP +7 m. However, the highest dunes reach to NAP +25 m. The western part of the area shows a great variability in dune height in particular. The dunes east of beach pole 4 consist of a sand-drift dike which has an elevation of approximately NAP +7 m. Between beach pole 3 and the 'Strandweg' an extensive swampy dune valley is located named the 'Lange Duinen Noord'.

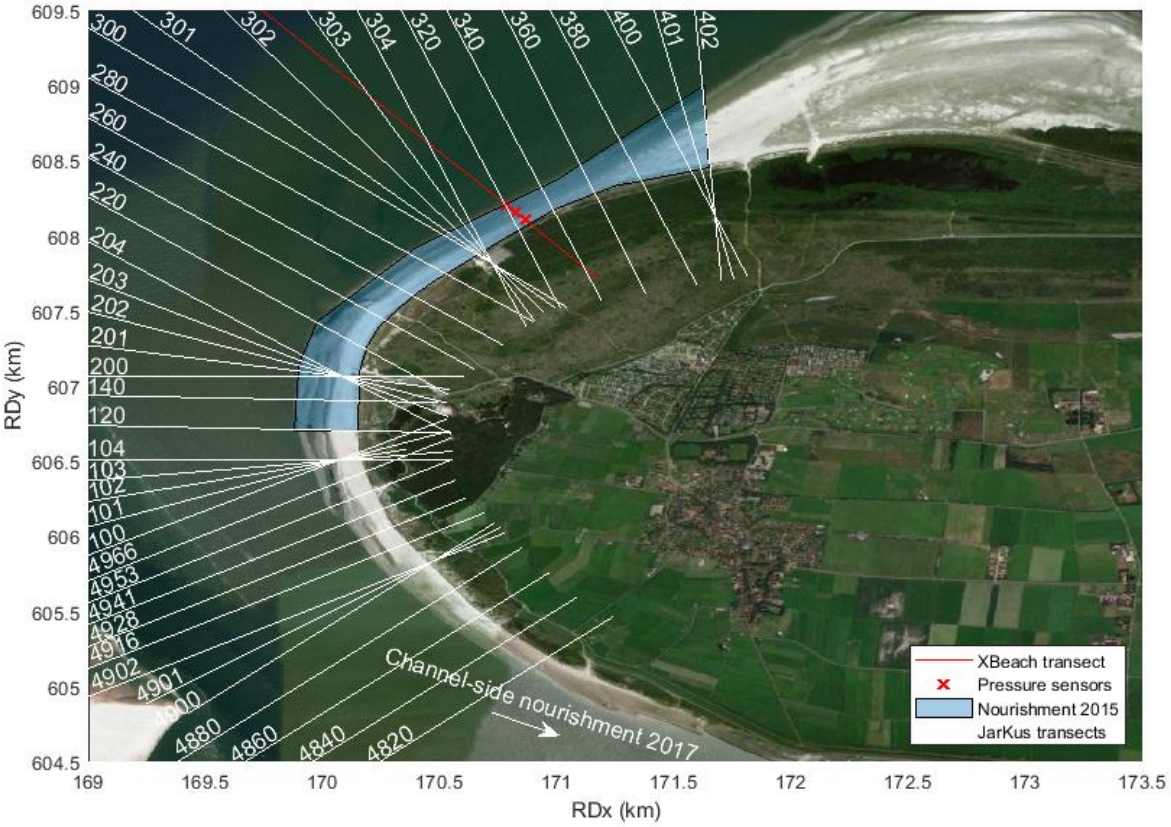

Figure 1.2. Aerial photo of Ameland Northwest.

1.2.3 Formation & development

The formation of the area is related to the closure of an ebb tidal delta channel when an ebb tidal delta shoal merged with the island. The merging of the shoal to the island formed a beach plain. The former shoreline is located landward of the 'Lange Duinen Noord'. In 1959 a sand-drift dike was constructed as outer dune row which changed the area between the new dike and the old dunes to a swamp. In the mid-1960s two small openings developed in the dunes at transect 4.0 and 4.4. Since 1970 these opening were left open, and seawater intrusion occurred during storm surges. Due to sand-drifting the openings were gradually filled and the intrusion of sea water is nowadays limited.

1.2.3.1 Large-scale development

The morphological situation in 2011 is shown in Figure 1.3. Here it can be seen that the Borndiep-Akkepollegat is clearly the dominant channel at the eastside along the west coast of Ameland. At the west side, along the Boschplaat, the channels Westgat (seaside) and Boschgat (basin) were located. The small channel in front of Ameland Northwest is named the Oostgat. The largest shoal on the ebb tidal delta was located north of the main channel. The Ameland tidal inlet shows cyclic behaviour where single and double channel systems alternate (Van der Spek en Noorbergen, 1992; Israël, 1998; Israël en Dunsbergen, 1999; Cheung et al. 2007). In the single-channel system the Borndiep is the main active channel. In the double-channel system also the Boschgat is active.

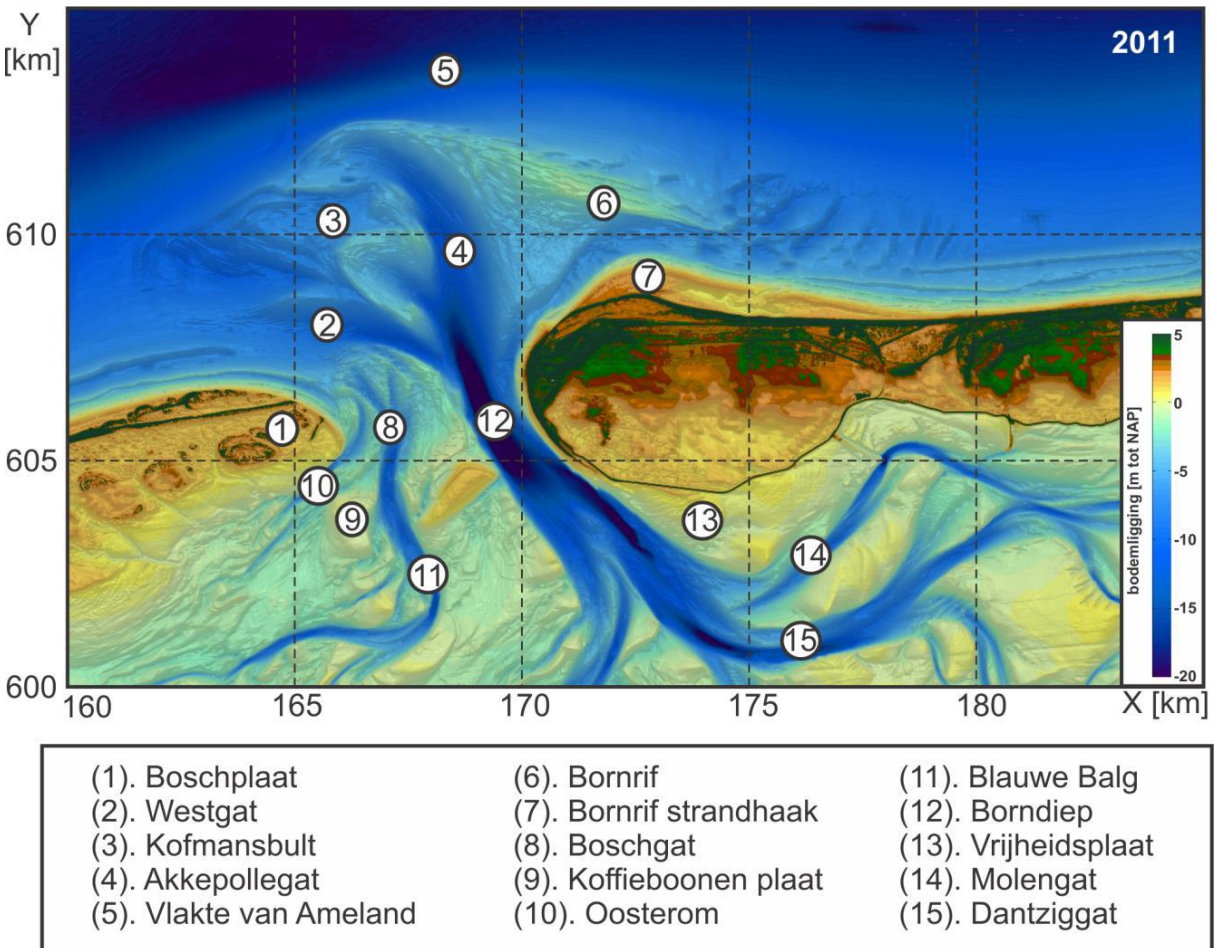

Figure 1.3. Overview of the main channels and shoals in the sea inlet of Ameland in 2011 (Elias & Bruens, 2013).

A schematization of the cyclicality of the Ameland inlet is shown in Figure 1.4. The duration of the cycle is 50 to 60 years. Because of the welding of the shoals, in this case the Bornrif, there is a periodic sand exchange with the western coast of Ameland. This can be seen in the formation of a spit. The welding and development of the Bornrif is an important factor in the development of the coast of Ameland Northwest. The Bornrif spit showed a decrease in volume of 20 million m^3 in the period 1982-2008. The erosion especially led to almost completely disappearance of the beach south of beach pole 4. This is caused by the relatively steep beach and the forcing of the Oostgat on the beach. Since 2008 the volume of the Bornrif spit increases again, but the south of beach pole 4 erosion continues (Figure 1.5). However, the Bornrif will merge more to the east and therefore it is not sure whether the sand will disperse to the area south of beach pole 4. According to Israel & Dunsbergen (1999) the welding of the Bornrif is expected around 2030. The erosion at Ameland West is related to the eastward migration of the Borndiep.

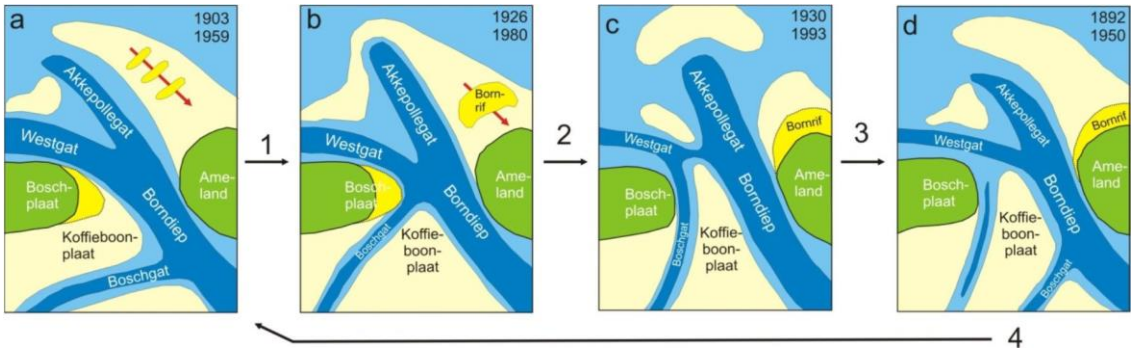

Figure 1.4. Cyclicality in the sea inlet of Ameland (Israel and Dunsbergen, 1999).

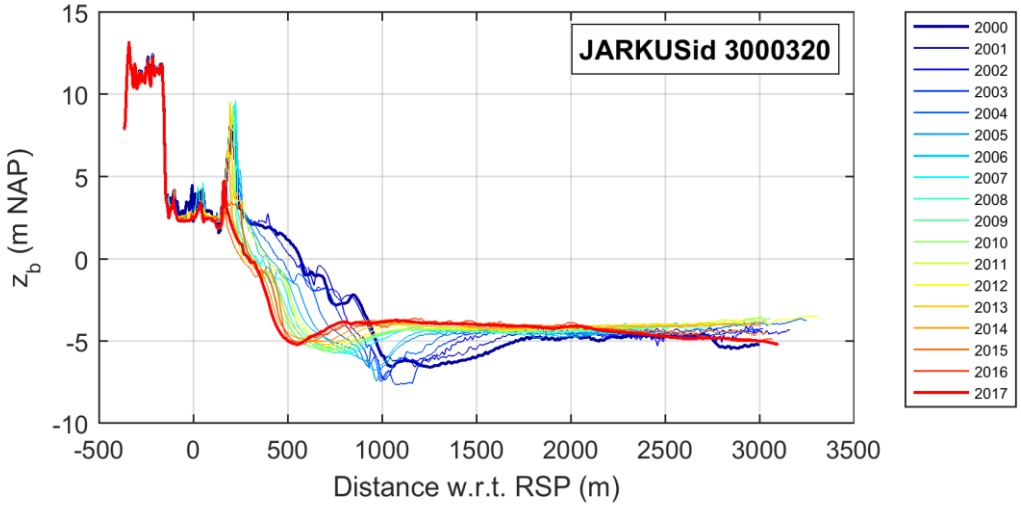

Figure 1.5. Bed elevation JarKus transect (3000)320 of 2000-2017.

1.2.3.2 *Nourishments*

The foreshore-beach-dune system at Ameland Northwest is affected by human intervention. In the last couple of years several nourishments were placed to protect and strengthen the Ameland beach. The nourishments are shown in Table 1.1. When studying the development of Ameland Northwest the effect of these nourishments on the hydrodynamics and morphodynamics should be taken into account. In the Borndiep southwest of transect (300)4820 a channel-side nourishment was placed in 2017.

Table 1.1. Nourishments at Ameland (North)west.

Year	Type	Begin transect	End transect	Length (m)	Volume (m³)
2004	Beach	3000200	3000320	1200	403636
2007	Beach	3000200	3000320	1200	303444
2007	Foreshore	3000195	3000302	1070	1201234
2010	Beach	3000200	3000400	2000	1888934
2015	Beach	3000140	3000402	2620	1300000

1.3 Aim of this study

The aim of this study is to determine the effect of the 2017/2018 storm season on the beach and dunes of Ameland Northwest. The data collected by the QRF will be used to give an overview of the hydrodynamics and morphodynamics during this storm season and its effect on the coast of Ameland Northwest. With the model XBeach these hydrodynamics and morphodynamics can be predicted. The XBeach model results are here validated with the measured data. Advice is provided for future monitoring and modelling.

The research questions and sub questions are the following:

- How did the morphology of Ameland Northwest change during the storm season of 2017/2018 and what caused this change?
  - *Which sequence of storms occurred in the storm season of 2017/2018?*
  - *What were the water levels, wave conditions and wind conditions related to the storm season of 2017/2018?*
  - *How did the morphology of the foreshore, beach and dunes change during the storm season of 2017/2018?*
- How do the XBeach model results (hydrodynamics and morphodynamics) compare to the measured hydrodynamics and morphodynamics?

2 Part 1: Analysis storm season 2017/2018

2.1 Introduction

Ten storm surges occurred during storm season of 2017/2018 (Table 2.1). A storm is classified as a storm surge when the water levels exceed the warning level ('waarschuwingspeil'). The high water levels exceeded the alarm level ('alarmeringspeil') during the storm surges of 28-29 October 2017, and 3-4 January 2018. These storm surges will be referred to as severe storm surges. Relatively many storm surges occurred in 2017/2018 as compared to earlier years (Table 2.2). This yielded useful QRF measurement data. The strong storm season led to a dune breach on 18 January 2018.
The hydrodynamics and meteorology related to the storm season are described in section 2.2 while the effect of the storm season on the foreshore-beach-dune system is described in section 2.3. Section 2.4 gives an overview of the hydrodynamics and morphodynamics during the storm season of 2017/2018.

Table 2.1. Storm surges occurring during the storm season of 2017/2018.

Storm surge #	Date
1	13 September 2017
2	5 and 6 October 2017
3	28 and 29 October 2017
4	10 November 2017
5	18 and 19 November 2017
6	8 and 9 December 2017
7	10 December 2017
8	3 and 4 January 2018
9	16 and 17 January 2018
10	1 and 2 February 2018

Table 2.2. Number of storm surges over the last 10 years.

Storm season	# of storm surges (warning level)	# of storm surges (alarm level)
2017/2018	10	2
2016/2017	6	1
2015/2016	9	0
2014/2015	7	2
2013/2014	6	1
2012/2013	2	0
2011/2012	14	0
2010/2011	4	0
2009/2010	2	0
2008/2009	6	0

2.2 Wind, waves & water level

2.2.1 Wind

Figure 2.1 shows the wind direction, mean wind speed and the maximum wind speed measured at Hoorn, Terschelling. During the last part of 2017 the wind direction was mainly directed west. In the first part of 2018 the wind direction was more variable and also winds from the east occurred. The storm surges mostly corresponded with winds from the NW and NNW. Only the storm surges in September 2017 and January 2018 had mainly winds from the west. During four of the storm surges the wind reached wind force 7 (moderate gale). The storms on 13 September 2017, and 3 and 4 January 2018 even reached wind force 9 (strong gale). It is interesting to see that the severe storm surge on 28 and 29 October 2017 only reached wind force 7. However, the maximum wind speed during this storm surge was large (~25 m/s). Furthermore, there were ten events which reached wind force 7, but were not classified as storm surges. In March 2018 there were also two events which reached stormy conditions (wave force 8). However, during these events the winds came from the east and therefore did not generate a storm surge.

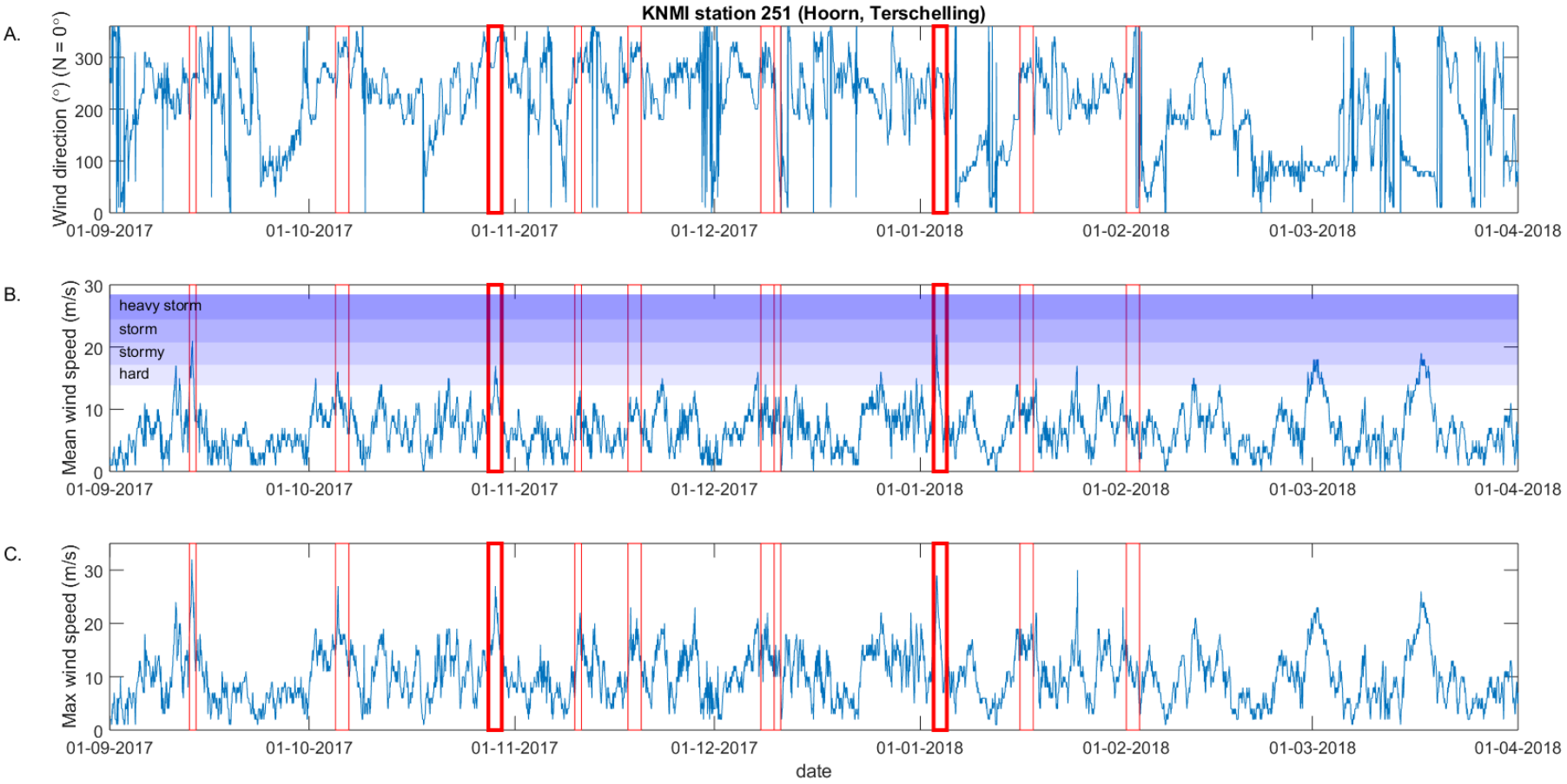

Figure 2.1. Wind direction (A), mean wind speed (B) and maximum wind speed (C) during the storm season of 2017/2018 measured by KNMI station 251 located at Hoorn, Terschelling. The red boxes indicate the storm surges. The thicker lines are the severe storm surges.

2.2.2 Waves

2.2.2.1 Offshore

Wave data was collected at several locations in the Ameland tidal inlet (Fig. 2.2). The wave buoys Amelander Zeegat – Boei 1-1 and 1-2 are located north of the ebb-tidal delta, the wave buoys Amelander Zeegat – Boei 2-1 and 2-2 are located on the edge of the ebb-tidal delta and the wave buoys Amelander Zeegat – Boei 3-1 and 3-2 are located near the tidal inlet. The wave data is available for every 10 minutes. Some wave buoys have been malfunctioning during the storm season 2017/2018.

Figure 2.3 shows the significant wave height H_{m0} from the different wave buoys. The highest wave events correspond with the storm surges. North of the ebb-tidal delta the waves were highest. During all storm surges the wave heights exceeded 4 meters. On 28 and 29 October 2017 the wave height exceeded 7 meters. At the edge of the ebb-tidal delta the waves were already considerably lower (< 3 m) because of the limited water depth. The high wave heights recorded by wave buoy Amelander Zeegat – Boei 2-1 end November 2017 and begin December 2017 are considered as incorrect spikes as the other wave buoys do not show these wave heights and the increases are abrupt. The wave heights at wave buoys Amelander Zeegat 2-1 and 2-2 are similar for all storm surges (2 - 2.5 m). At wave buoy Amelander Zeegat – Boei 3-1, which is located closest to Ameland Northwest, the wave heights during storm surges generally range between 1.5 – 2 m. The wave direction during storm surges was mainly NW (Fig. 2.4). The waves refract to shore normal directions when propagating shoreward. The wave refraction is affected by the complex bathymetry of the ebb tidal delta and the curvature of the islands. The peak wave period was highest during the peak of the storms and ranged between 9 and 17 s north of the ebb-tidal delta (Fig. 2.5). This was similar for all wave buoys.

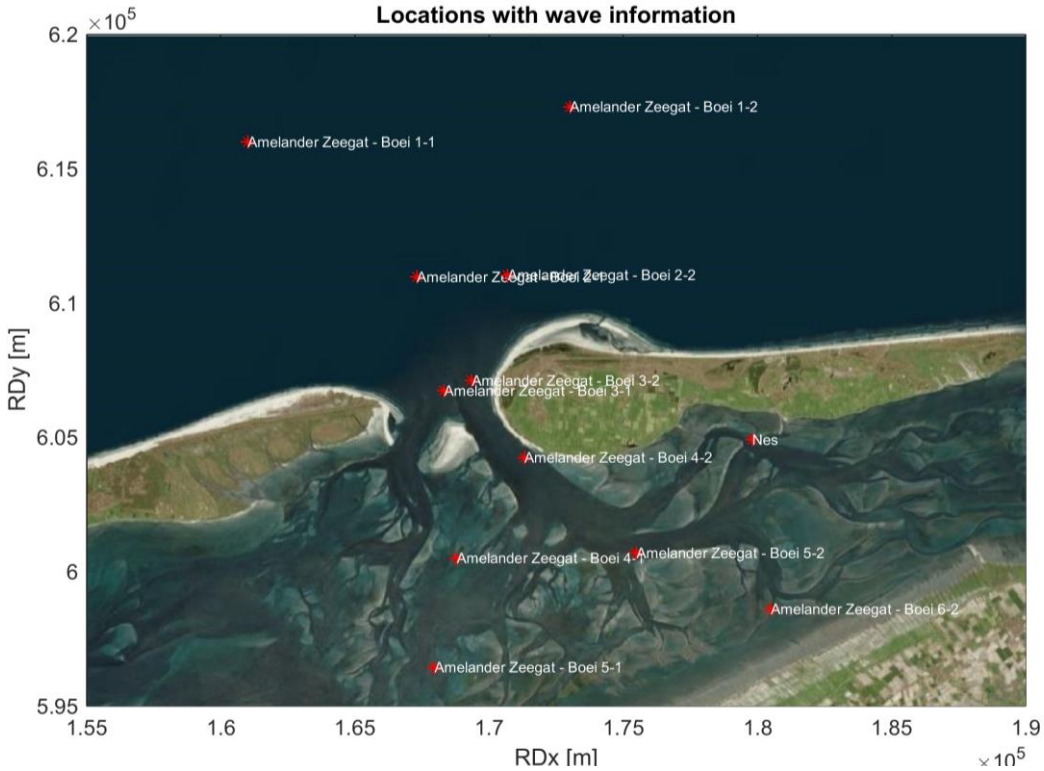

Figure 2.2. Locations of the wave buoys.

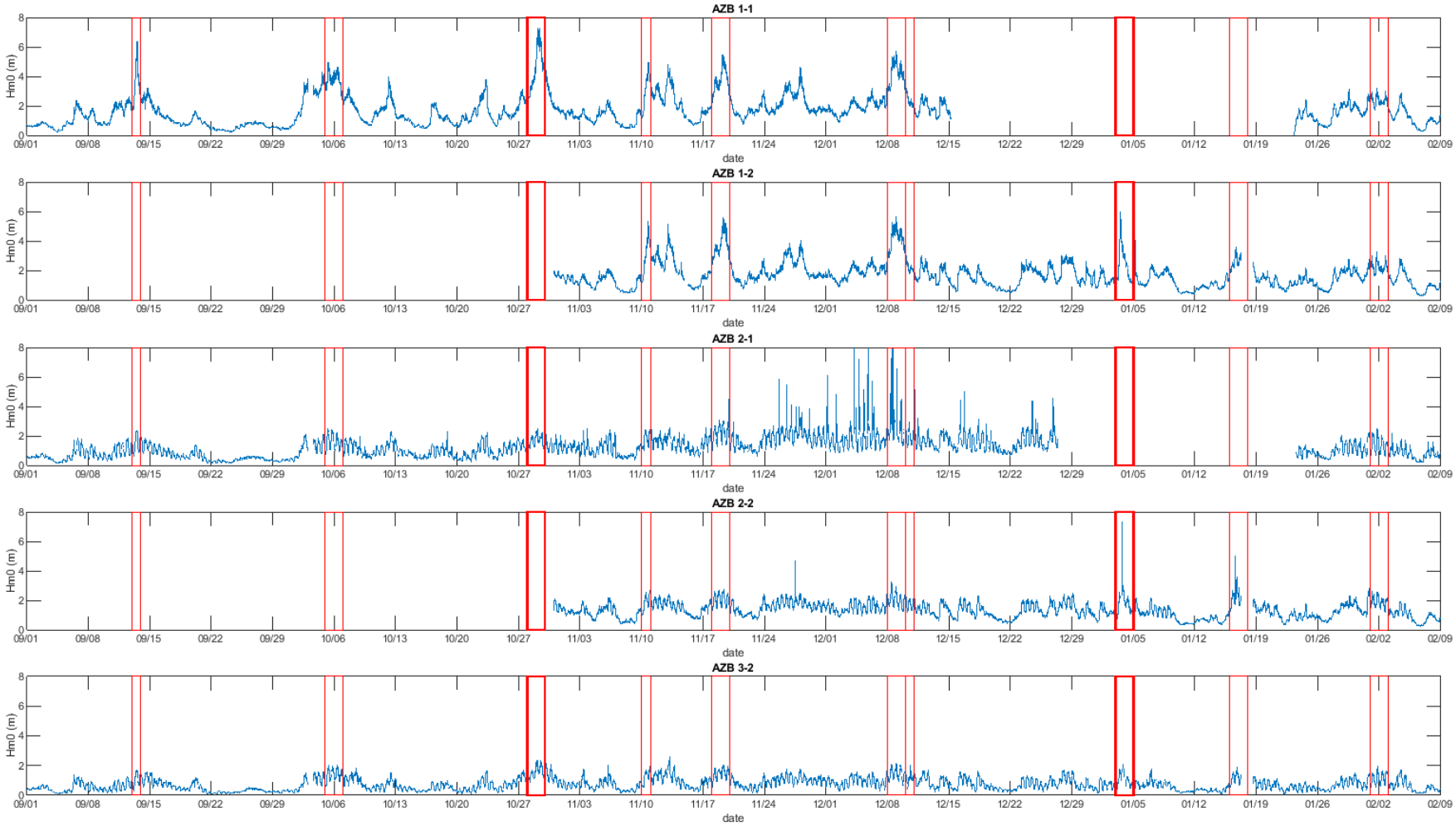

Figure 2.3. The significant wave height H_{m0} measured by Amelander Zeegat – Boei 1-1, 1-2, 2-1, 2-2 and 3-2 between 1 September 2017 and 9 February 2018. The red boxes indicate the storm surges. The thicker lines are the severe storm surges.

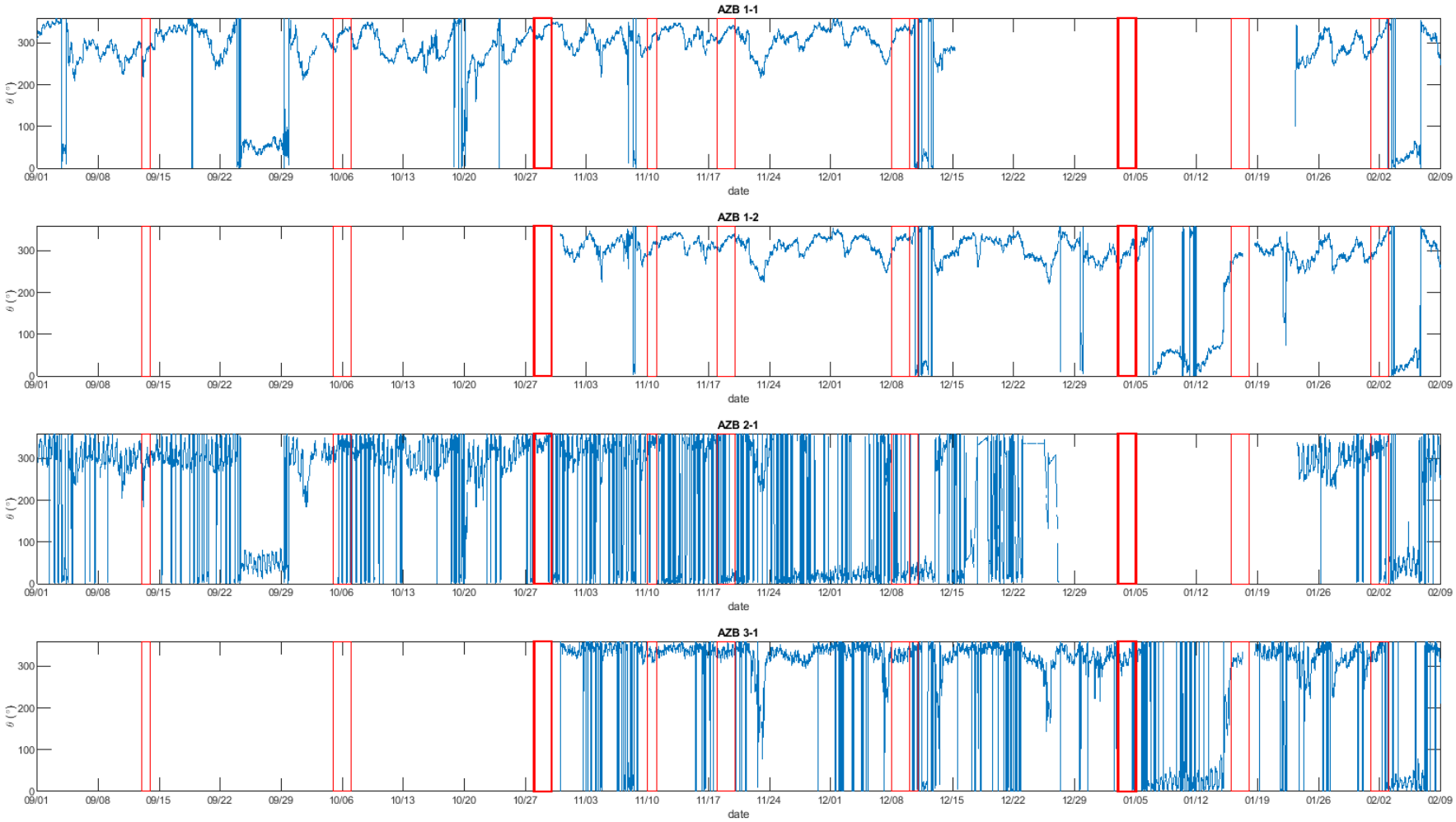

Figure 2.4. The wave direction θ measured by Amelander Zeegat – Boei 1-1, 1-2, 2-1 and 3-1 between 1 September 2017 and 9 February 2018. The red boxes indicate the storm surges. The thicker lines are the severe storm surges.

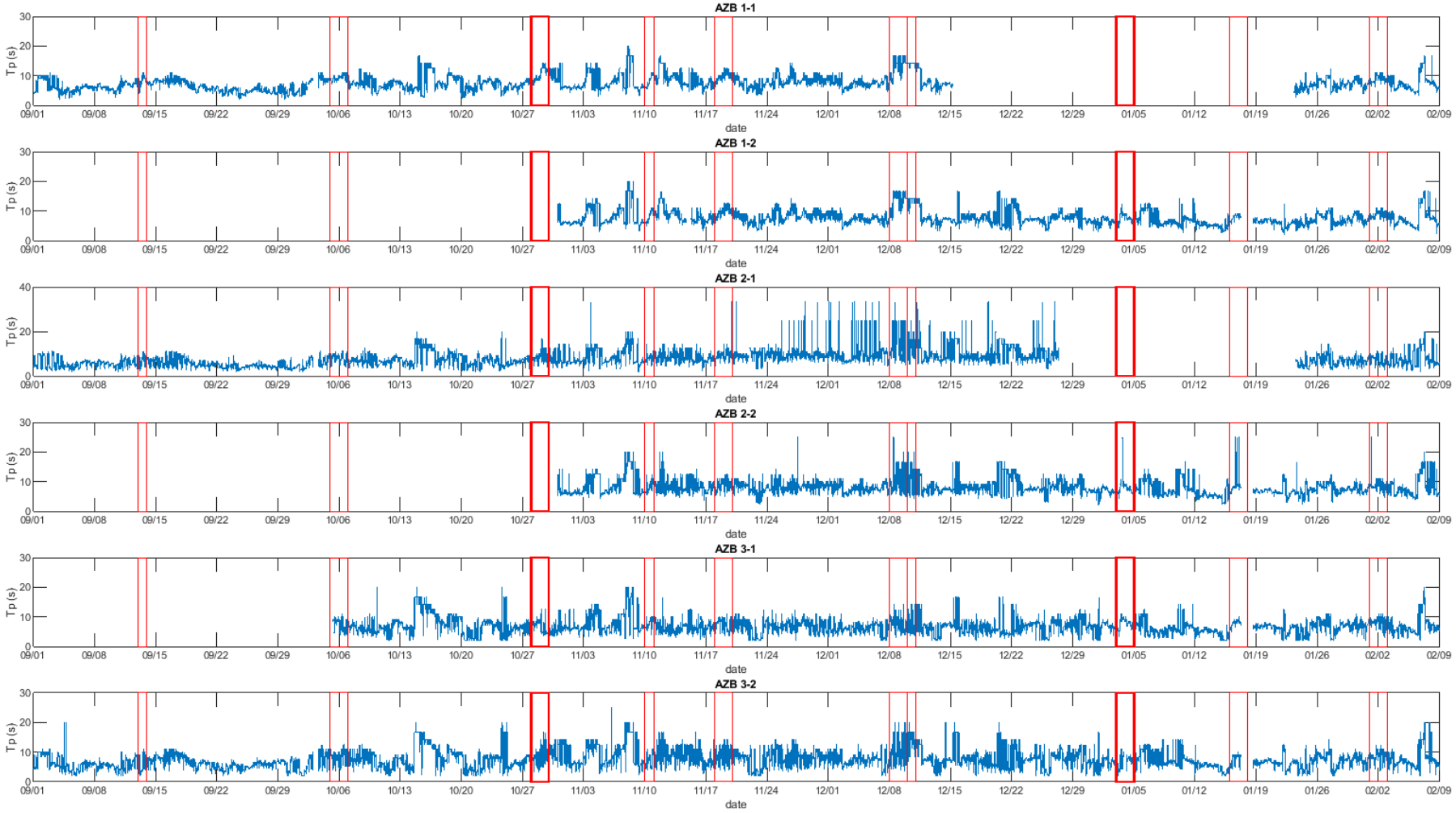

Figure 2.5. The peak wave period T_p measured by Amelander Zeegat – Boei 1-1, 1-2, 2-1, 2-2, 3-1 and 3-2 between 1 September 2017 and 9 February 2018. The red boxes indicate the storm surges. The thicker lines are the severe storm surges.

2.2.2.2 Nearshore

The QRF placed pressure sensors along a transect perpendicular to the dunes on the beach of Ameland Northwest to monitor waves and water levels on the beach. The pressure sensors have a sampling frequency of 6 Hz. The locations of these sensors are shown in Table 2.3, Figure 2.6 and Figure 2.11. One sensor was placed below low water, one sensor was placed at about mean sea level and one sensor was placed above high water. The sensors measured between 21 September 2017 and 4 April 2018 and were serviced between 17 November 2017 and 11 December 2017. During the storm season of 2017/2018 erosion occurred on the beach. The bed level decreased by 0.76 m at sensor 55180, 0.72 m at sensor 55181 and 1.13 m at sensor 55182. It should be noted that the sensor initially mounted at a few decimetre above the bed. This means that when water reached the cross-shore location of the sensor, it was only registered when the water level was high enough to reach the sensor height. We should also note here that the water depth plotted in the figures was not corrected for the change in bed level during the storm season.

Figure 2.7 shows the wave height, wave spectrum peak period and water depth measured at sensor 055180. This sensor was located below mean low water level (MLW) and was therefore always submerged. During calm conditions the wave height was around 0.5 m. In the period between October 2017 and February 2018 the wave heights were highly variable over time. In the following period conditions were calmer. In the whole period the water depths varied between approximately 0.5 m and 3.5 m. Low wave conditions often corresponded to low water depths.

Most of the storm surges logically correspond with larger wave heights (~2 m) and larger water depths (~3 m) on the beach (Fig. 2.7). The storm surges of 5-6 October 2017, 28-29 October 2017, and 3-4 January 2018 showed wave heights above 2 meters and water depths larger than 3 meters. Around 11 February 2018 also large waves occurred (up to 2 m) with large water depths (up to 3 m) but this period was not classified as a storm surge. The wave peak periods of the storm surges mainly varied between 8 and 12 s.

The wave heights measured at the middle sensor placed at about mean sea level (MSL) were smaller than at the lowest sensor because of the dissipation of wave energy. The wave heights during the storm surges varied here between 1.2 and 1.6 m with a corresponding peak wave period of 10 to 15 s. The water depth during the storm surges exceeded 2 m. The decrease in wave height was larger in the first part of the storm season than in the second part of the storm season. This is likely caused by beach erosion and therefore less wave dissipation. The decrease in water level was similar.

The sensor placed above mean high water (MHW) was only submerged during storms. The measured data mostly correspond to the storm surges. The storm on 11 February 2018 also reached the upper part of the beach. The wave heights mainly ranged between 0.4 m and 0.8 m, but during the storm of 3-4 January 2018 the wave height reached 1.1 m. The corresponding peak wave periods ranged between 10 s and 15 s. The water depths ranged between 0.4 m and 1.2 m. The storm of 3-4 January 2018 was clearly the strongest storm. The high water level and large wave heights during this storm probably led to the most erosion. Again, the decrease in wave height between sensor 55181 and sensor 55182 was larger in the first part of the storm season than in the second part of the storm season. The decrease in water depth was larger in the first part of the storm season compared to the last part of the storm season.

Table 2.3. Serial numbers, locations and elevations of the sensors before and after the storm season 2017/2018.

Serial number	x (m RD)	y (m RD)	z bottom sensor above bed before (m NAP)	z bed before (m NAP)	z bottom sensor above bed after (m NAP)	z bed after (m NAP)	Bed level change (m)
55180	170784.5	608202.5	0.29	-1.39	1.05	-2.15	-0.76
55181	170825.6	608151.6	0.28	-0.18	1.00	-0.90	-0.72
55182	170865.4	608101.9	0.13	1.40	1.26	0.27	-1.13

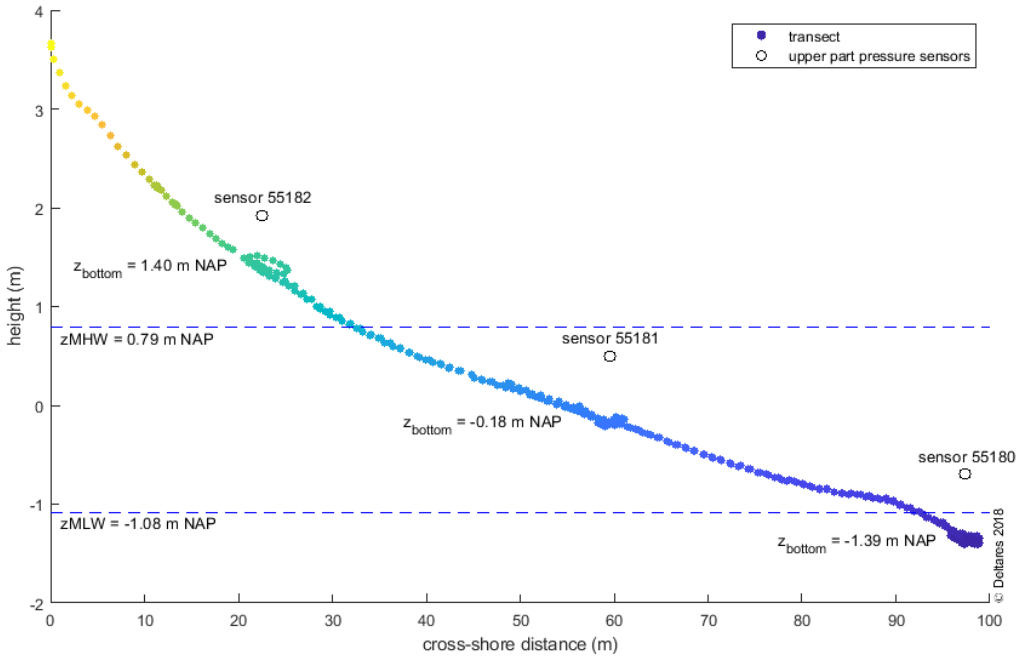

Figure 2.6. The locations of the pressure sensors on the transect.

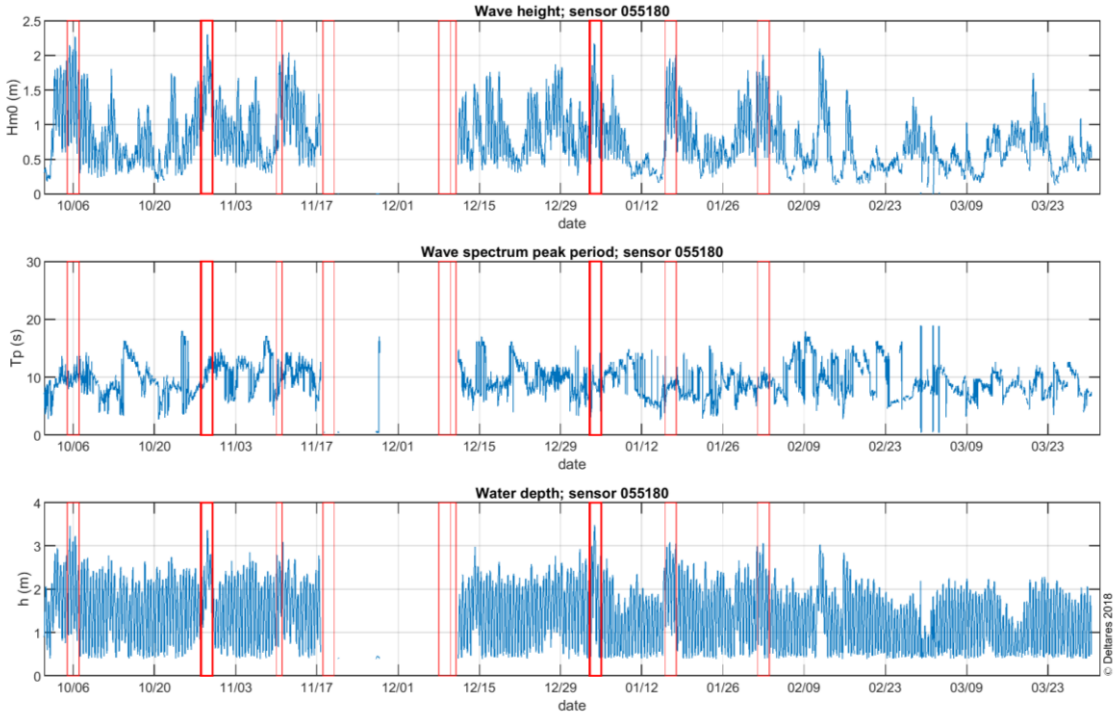

Figure 2.7. Wave height (A), wave peak period (B) and water depth (C) at sensor 055180. The red boxes indicate the storm surges. The thicker lines are the severe storm surges.

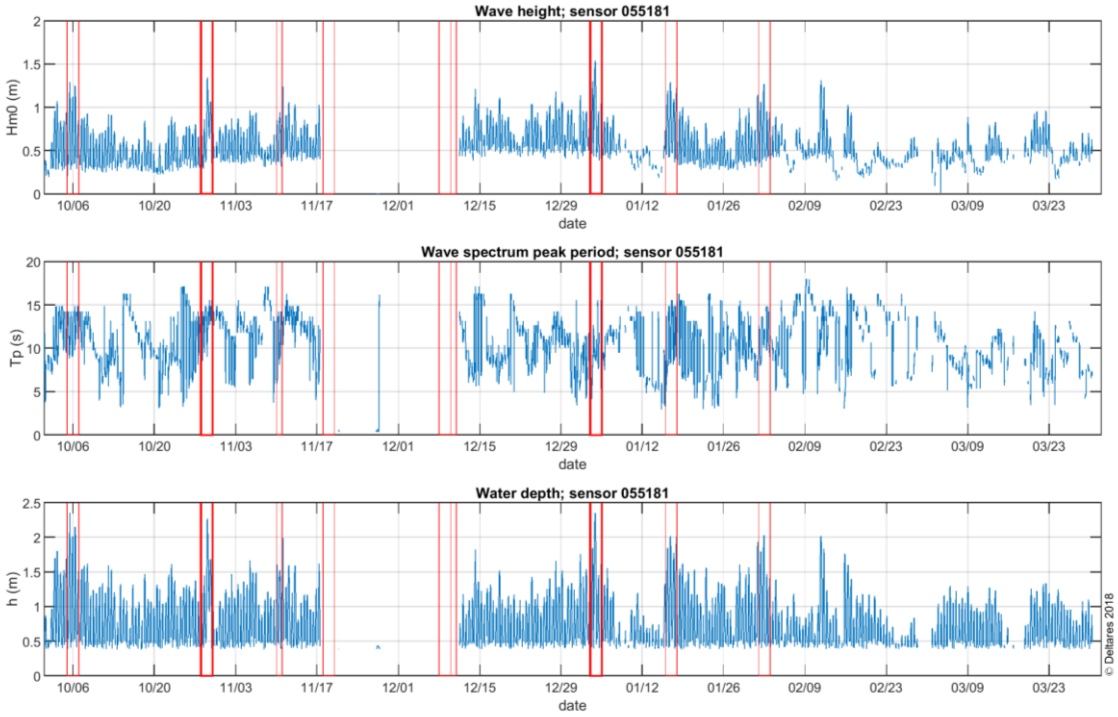

Figure 2.8. Wave height (A), wave peak period (B) and water depth (C) at sensor 055181. The red boxes indicate the storm surges. The thicker lines are the severe storm surges.

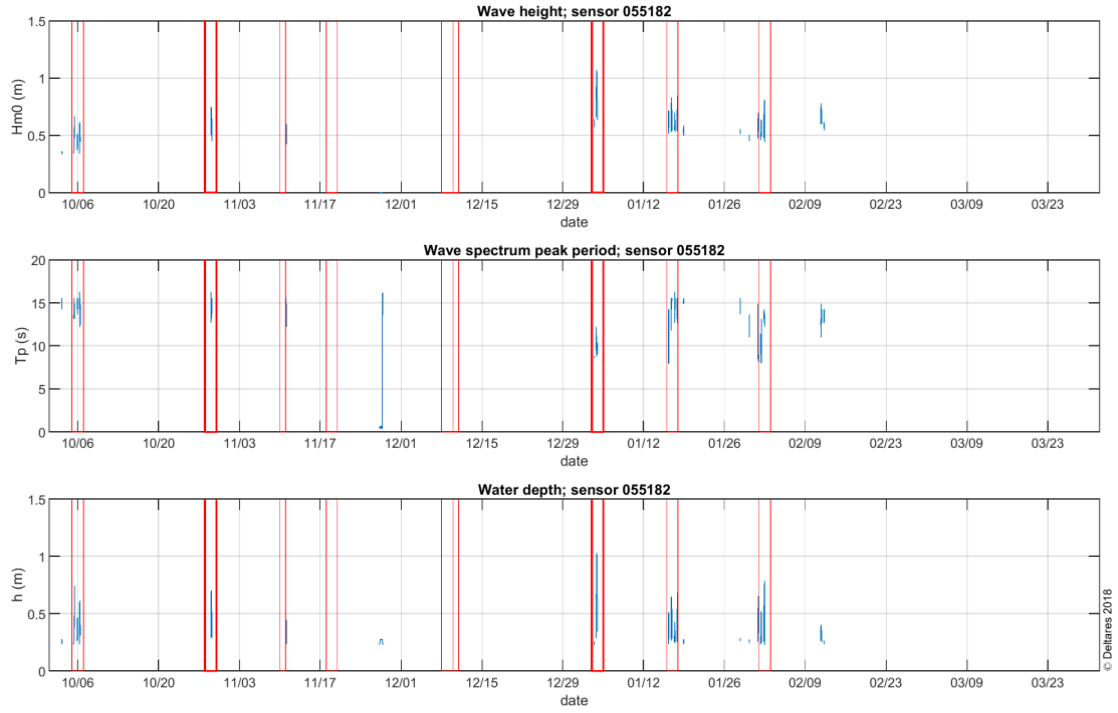

Figure 2.9. Wave height (A), wave peak period (B) and water depth (C) at sensor 055182. The red boxes indicate the storm surges. The thicker lines are the severe storm surges.

2.2.3 Water level

Water levels were measured at wave buoy Wierumergronden (Fig. 2.10). This wave buoy is located 3 km north of East Ameland (Fig. 2.11). Where the water levels at the pressure sensors did show high water levels for the storm conditions this is not the case for the offshore water levels. Of course, wind and wave set-up is only present at the beach. During neap tide the tidal range is approximately 1.6 m and during spring tide the tidal range is approximately 2.2 m. The reason for the peaks in water level is unknown.

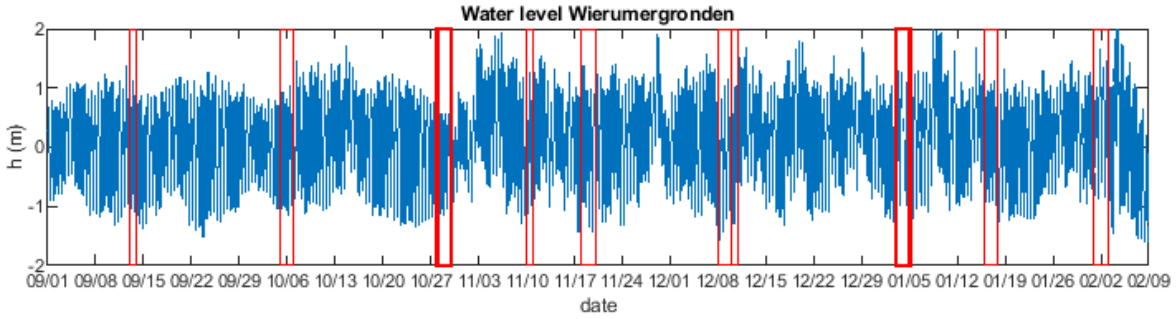

Figure 2.10. Water level measured at wave buoy Wierumergronden. The red boxes are the storm surges.

Figure 2.11. Location of wave buoy Wierumergronden.

2.3 Morphology

Figure 2.12 and 2.13 show the bed elevation of the foreshore, beach and dunes before and after the storm season, respectively. The bed elevation of the beach and dunes was obtained with LiDAR on 22 September 2017 (before storm season) and 26 January 2018 (end storm season) with a resolution of 2 m x 2 m. The bed elevation of the foreshore was measured after the storm season (12 March 2018) with a multibeam echosounder (resolution: 1 m x 1m). To compare this data with the bed elevation before the storm season, the bed elevations of the JarKus transects is used which were collected in February 2017. To determine the impact of the storm season on the foreshore-beach-dune system, the change in bed elevation was determined (Fig. 2.14 & 2.15).

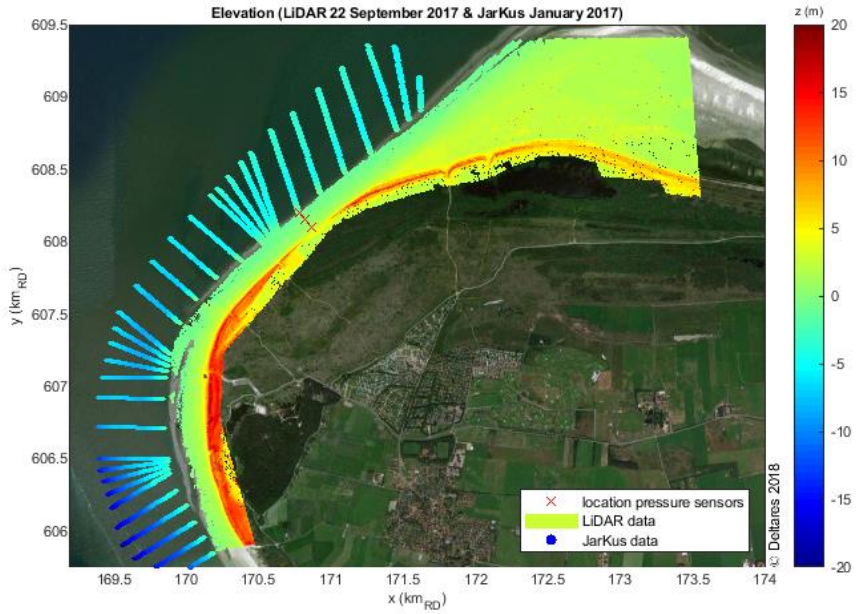

Figure 2.12. Bed level elevation of the beach and dunes (LiDAR, collected on 22 September 2017), and the foreshore (JarKus, collected in February 2017).

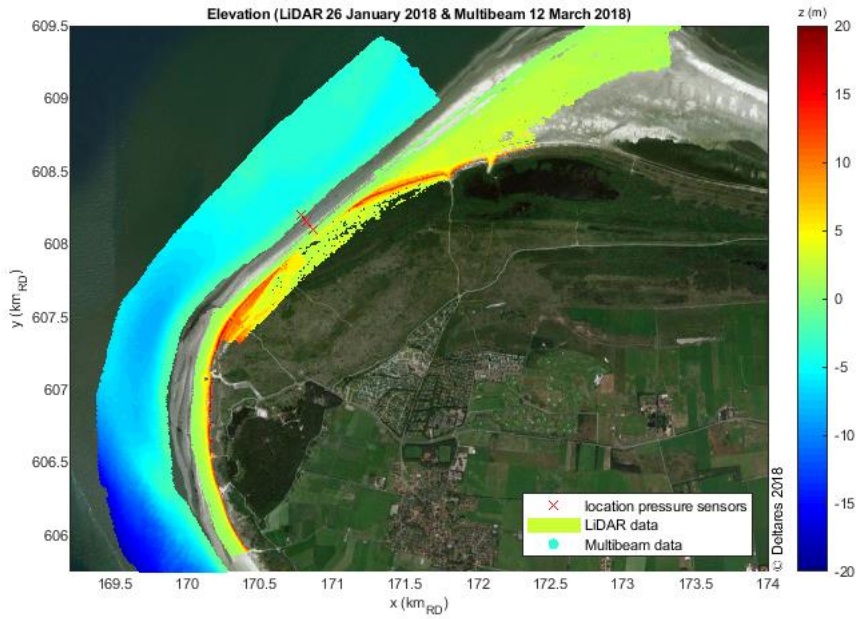

Figure 2.13. Bed level elevation of the beach and dunes (LiDAR, collected on 26 January 2018), and the foreshore (Multibeam, collected on 12 March 2018).

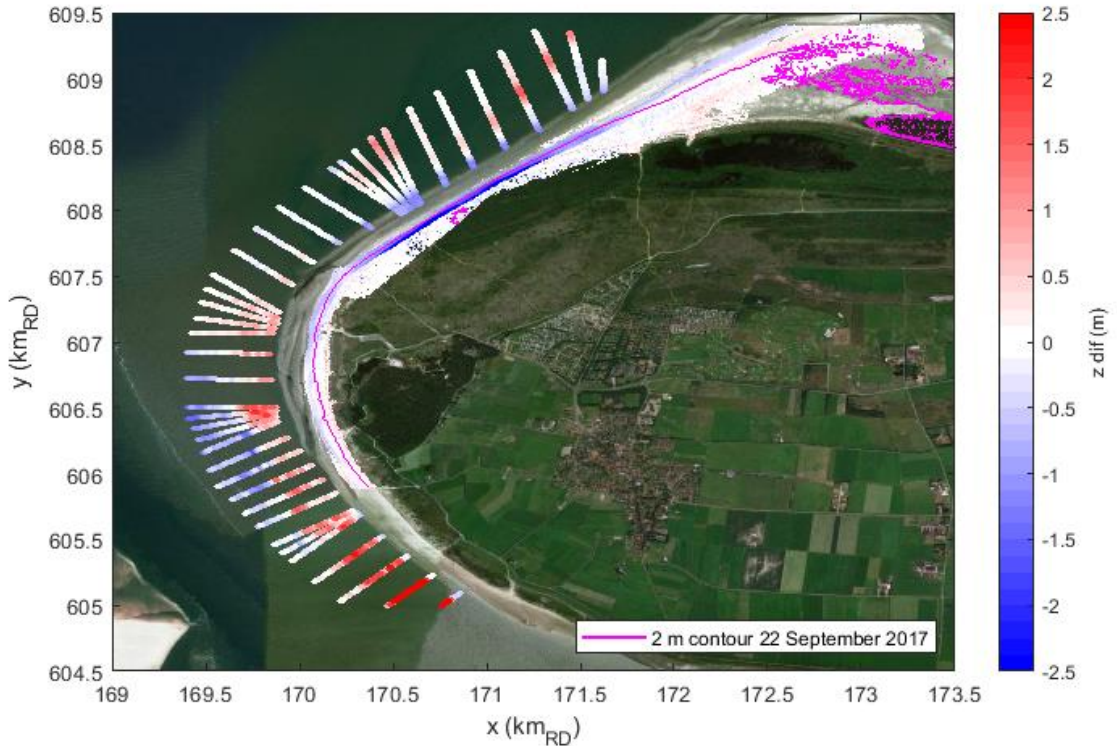

Figure 2.14. Change in bed level elevation of the beach and dunes between 22 September 2017 (LiDAR) and 26 January 2018 (LiDAR), and of the foreshore between February 2017 (JarKus) and 12 March 2018 (Multibeam). Red represents deposition and blue erosion. The yellow circle indicates the breakwater.

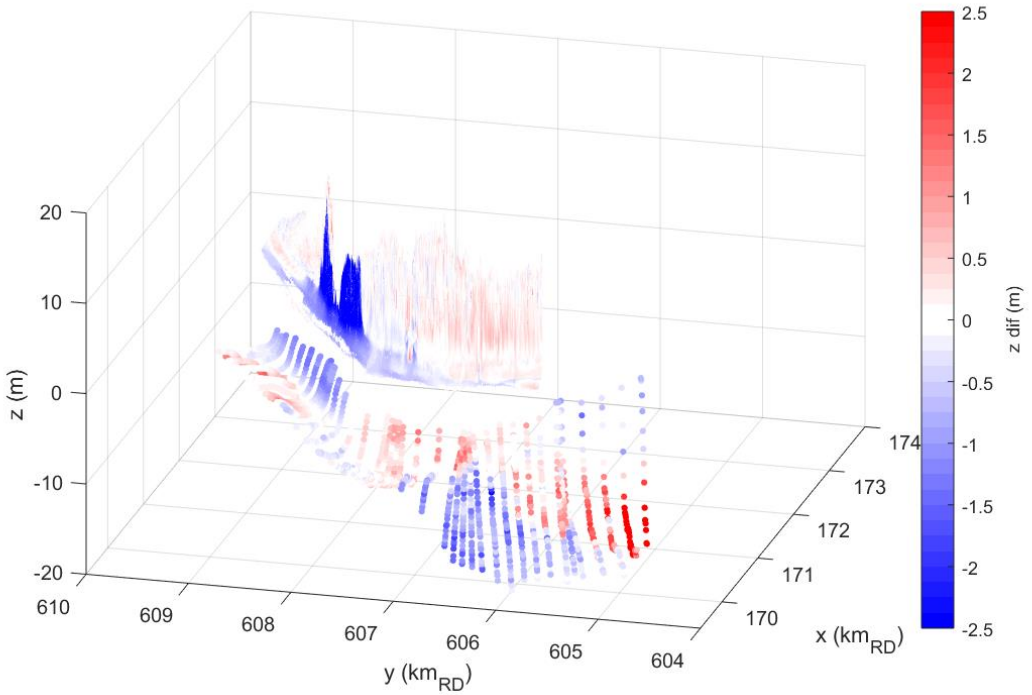

Figure 2.15. Bed level elevation of the beach and dunes on 22 September 2017 (LiDAR), and foreshore in February 2017 (JarKus). The color represents the change of bed elevation of the beach and dunes between 22 September 2017 (LiDAR) and 26 January 2018 (LiDAR), and of the foreshore between February 2017 (JarKus) and 12 March 2018 (Multibeam). Red represents deposition and blue erosion.

2.3.1 Beach & dunes

The bed level elevation covered by the LiDAR varies between approximately NAP -1.08 m (the mean low water line) and approximately NAP +12 m (dune crest). At the location where the pressure sensors were placed, the dunes were generally lower than the surrounding areas, namely around NAP +4 m. Approximately four months later the second LiDAR survey was conducted. Unfortunately, the survey could not be conducted during low water and therefore the bed level elevation varies between mean sea level and approximately NAP +12 m (dune crest).

Figure 2.14 and 2.15 clearly show that erosion (up to 10 m in 4 months) took place along the whole beach which was largest for the dunes landward of the pressure sensors. In this area the erosion was especially concentrated above the NAP +2 m contour (elevation dune foot) of 22 September 2017 which indicates especially dune erosion took place in this area. This can also be seen in the change of bed elevation at the sensors where the most landward sensor shows the most erosion. A dune breach occurred during the storm of 18 January 2018. It is interesting to see that southwest and northeast of this area the erosion mainly took place below the NAP +2 m contour. The magnitude of the erosion was also lower. More to the northeast in the direction of the so called green beach (‘groene strand’), sedimentation occurred.

The erosion in previous years was mainly focussed on the foreshore (Fig. 1.5). Despite of the nourishments which were placed at the beach of Ameland Northwest the foreshore kept retreating. In these years the dune erosion was limited; however it seems that in this storm season the foreshore was eroded sufficiently so that the waves were now able to erode the dunes. This already led to a dune breach and it is expected that dune breaches will happen more often in the upcoming years.

2.3.2 Foreshore

The tidal channels on the foreshore consist in the southeast of the area of the Borndiep tidal channel and in the north of the smaller Oostgat tidal channel. However, the Oostgat tidal channel is not a typical tidal channel with clear flood and ebb currents (Nederhoff et al., 2016). The higher area west of this channel is a part of the Bornrif (see also Figure 1.3). The Bornrif has been migrating towards the coast and therefore the Oostgat became narrower in the last couple of years and is forced on the beach of Ameland Northwest. The narrowing can also be seen in Figure 2.16. The multibeam data shows bed levels varying between approximately NAP -20 m (Borndiep) and NAP -1 m (close to the beach).

In the southwest of the study area very high sedimentation rates are present (up to ~8.5 m in approximately a year). Along the coast northwest of this area the sedimentation rates were lower up to JarKus transect (3000)240. More seaward of this sedimentation, erosion occurred. Along the beach northeast of JarKus transect (3000)240 also erosion took place (up to ~1.4 m in approximately a year). The part of the Bornrif seaward of this area shows sedimentation rates up to ~1.3 m in approximately a year.

The high sedimentation rates located near the Borndiep can be explained by the placement of a channel-side nourishment east of JarKus transect 3004840 which was placed in autumn 2017 (Fig. 2.17). The sand of this nourishment probably migrated to the northwest, but seems to stop around JarKus transect (3000)420. This could be related due to the presence of a breakwater (Fig. 2.14 & 2.18) which blocks the alongshore current and sediment transport. However, this could not be said with certainty because no data is available about the origin of the sediment. Northeast of this breakwater foreshore and beach erosion occurred. The mean

total transport along the coast Ameland Northwest is directed in southwestern direction (Nederhoff et al., 2016). Therefore, the large amounts of sand which are eroded at the beach of Ameland Northwest are transported to the Borndiep which then transports the sand to the outer part of the ebb tidal delta. The sedimentation more seaward in this area is related to onshore migration of this part of the Bornrif (Fig. 2.16). The erosion in the southwest of the study area is related to the presence of the Borndiep.

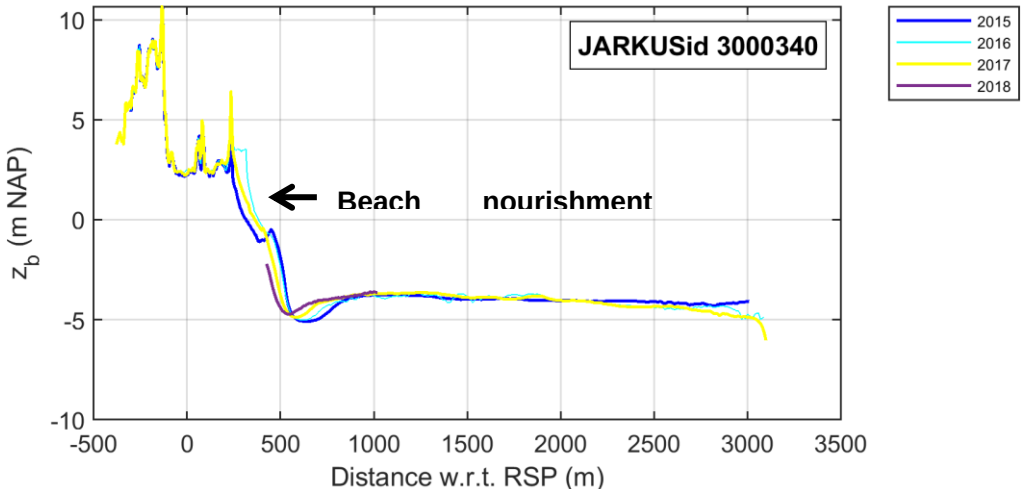

Figure 2.16. Bed elevation JarKus transect (3000)340 of 2015, 2016 and 2017. The purple line shows the bed elevation in 2018 collected with the multibeam.

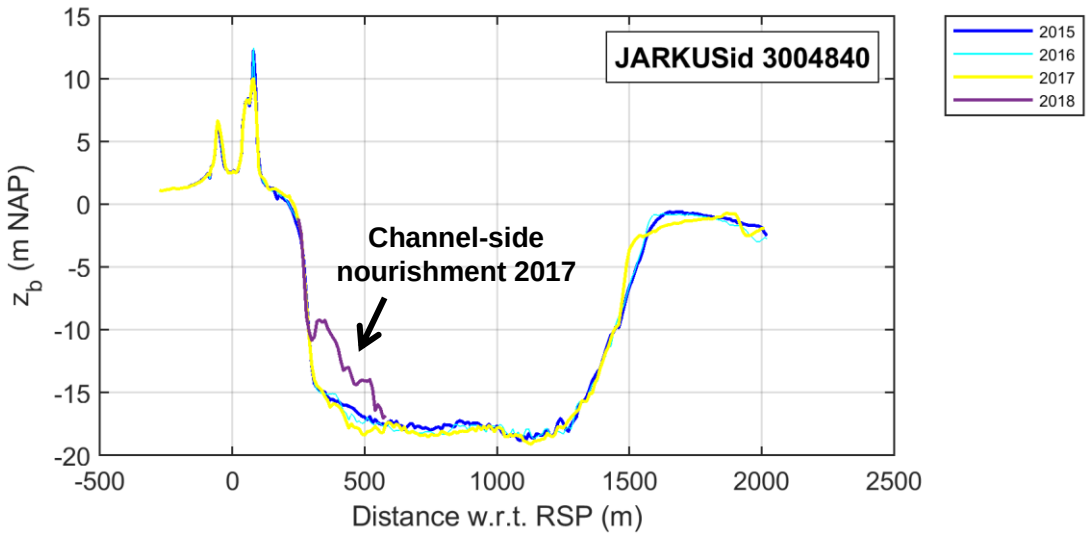

Figure 2.17. Bed elevation JarKus transect (3000)340 of 2015, 2016 and 2017. The purple line shows the bed elevation in 2018 collected with the multibeam.

Figure 2.18. Break water near JarKus transect 3000240 at Ameland West. The break water clearly extends more seaward than the adjacent areas.

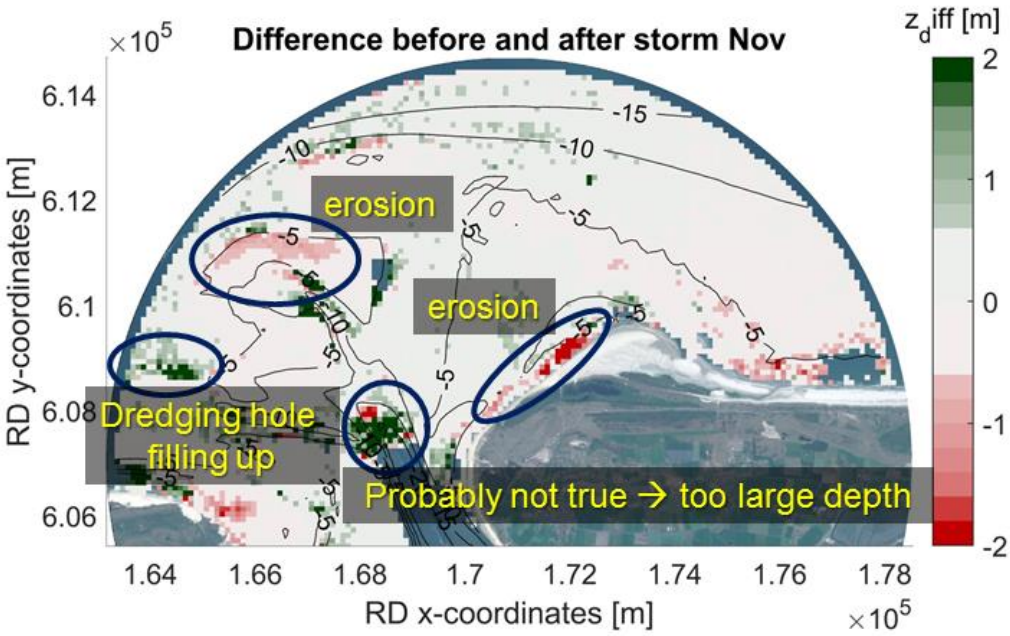

Figure 2.19. Bed level change determined with XBand radar for the month November.

At the lighthouse of Ameland an X-bandradar is located. With a relatively new technique the bed elevation can be determined from these X-band radar images. Figure 2.19 shows the bed elevation change after the storm period of November determined from X-band radar images. Clearly visible is the erosion above the NAP -5 m contour at the northwest side of Ameland. The advantage of this technique is that it has a high resolution in time compared with multibeam surveys. However, the spatial resolution is worse. The other available bed level elevations available for this study were considered as unreliable and are therefore not used for further research.

2.4 Summary hydrodynamics and morphodynamics during storm season 2017/2018

2.4.1 Hydrodynamics

In the storm season of 2017/2018 a total of ten storm surges occurred, which makes it a relatively energetic storm season. Two of these storm surges exceeded the alarm level. All storm surges and the related characteristics are summarized in Table 2.4.

The first storm surge occurred on 13 September 2017. North of the ebb-tidal delta the wave height varied between 2.7 and 6.4 m, the wave spectrum peak period ranged from 4 to 11 s and the wave direction was west. The main wind came from the SW/W and reached storm conditions. Unfortunately, the storm occurred before the pressure sensors were installed. However, this storm was accompanied by very high offshore wave heights (up to 6.4 m) and was probably very important for the first erosion of the beach.

The second storm occurred on 5 and 6 October 2017 and had wave heights of 2.6 – 5.0 m and a peak wave period between 7 and 11 s north of the ebb-tidal delta. The waves came from the SSW to NNW. Although the offshore wave height was relatively low for a storm, the wave height was relatively high on the beach. The wave height at sensor 55180 ranged between 2.1 and 2.3 m during high tide with a peak wave period between 8 and 14 s. At the second sensor the wave height decreased to 1.1-1.3 m and the peak wave period was 14-15 s. At the sensor closest to the dunes, the wave height decreased further to 0.6-0.7 m with a wave peak period of 16 s. The water depth was about 3.1-3.5 m at the lowest sensor and 0.6-0.9 m at the highest sensor. The wind direction varied between NWW and N with mean wind speeds reaching up to 16 m/s.

The third storm occurred on 28 and 29 October and exceeded the alarm level. The offshore wave height was 3.2-7.3 m with a peak wave period of 7-14 m north of the ebb-tidal delta. This wave height was the highest during this storm season. The waves came from the NW/NNW. Waves on the beach reached values between 1.7 to 2.3 m at the lowest sensor which was similar to the other storm surges. The corresponding peak wave period was 8-14 s. The wave height was 0.9-1.3 m (T_p = 14-16 s) at the middle sensor and 0.8 m (T_p = 16 s) at the highest sensor. The water depth was 2.5-3.4 m at the lowest, 1.5-2.3 m at the middle and 0.9 m at the highest sensor.

The fourth storm this storm season occurred on 10 November 2017, but was a relatively calm one. North of the ebb-tidal delta the offshore wave height varied between 2.2 and 5.0 m, the wave peak period was 6-11 s and the waves came from the NWW to NW. The wave height on the beach at the lowest sensor was also lower compared to other storms (1.9-2.0 m with T_p = 7-13 s). The wave height was 0.9-1.2 m (T_p = 14 s) at the middle sensor and 0.6 m (T_p = 16 s) at the sensor located highest on the beach. The water depth was 2.6-3.1 m at the most seaward sensor, 1.5-2.0 m at the sensor around mean sea level and 0.6 m at the most landward sensor. Winds came from the W/NW and reached a mean wind speed of 13 m/s.

The fifth storm occurred on 17-18 November 2017. The offshore wave height was 2.2-5.0 m with a peak wave period of 6-11 s. The waves came from the NWW/NNW and the wind came from the W/NW. The mean wind speed was 6-12 m/s. For this storm no nearshore wave data was available due to servicing of the pressure sensors.

The sixth storm occurred on 8 and 9 December 2017. The waves came from the NWW to NNW and had heights of 3.4-5.7 m with a peak wave period of 7-17 s. The mean wind speeds

varied between 6 and 14 m/s and the wind came from the W to NNW. For this storm no nearshore wave data was available due to servicing of the pressure sensors.

The seventh storm occurred on 10 December 2017. The offshore wave heights varied between 1.8-3.0 m which is relatively low. The waves came from the NNW to N and had a peak wave period of 13-14 s. The wind direction deviated from the other storm surges and ranged from E to SSW. The wind speed varied between 6 to 12 s. For this storm no nearshore wave data was available sue to servicing of the pressure sensors. The impact of this storm was likely minor for Ameland because of the low wave height. The fifth, sixth and seventh storm were relatively calm compared to the more severe storms at the beginning of the season.

The eighth storm occurred on 3 and 4 January and exceeded the alarm level. This storm showed the highest wind speeds (10-22 m/s). The wind direction was SWW to W. The offshore waves were also high (1.8 – 6.0 m), had a peak wave period of 4-12 s and came from the W to NNW. Near the beach the wave heights decreased to 1.6 – 2.2 with a peak wave period of 4-14 s. The wave height and peak wave period changed to 1.0-1.5 m and 13-16 s at the sensor in the intertidal zone and 0.8-1.1 m and 12 s at the sensor above high water, respectively. This was the highest wave height recorded by the sensor located highest on the beach; also the peak wave period deviated from the other storms. The water depth showed a similar trend. Compared to other storms the wave height was similar at the sensor in the subtidal zone (3.0-3.5 m) and at the sensor intertidal zone (1.5 -2.3 m). However, the water depth at the sensor in the supratidal zone was higher than during other storms (0.7-1.7 m). This storm probably played an important role in the erosion of the dunes during this storm season.

The ninth storm occurred on 16 and 17 January 2018. The offshore wave height was low (2.0 – 3.6 m). The peak wave period was also low (6-9 s) and the wave direction was W-NW. However, the wave height near the beach was similar to the other storms (1.8-2.2 m). The corresponding peak wave period was 5-10 s. On the intertidal beach the wave height was 1.1-1.3 m with a peak wave period of 14-16 s and on the supratidal beach the wave height was 0.7-0.9 m with a peak wave period 15-16 s. The water depth was 2.8 – 3.1 m at the sensor in the subtidal zone, 1.7-2.0 m at the sensor in the intertidal zone and 0.6-0.8 m at the sensor in the supratidal zone. The winds came from SSW to NWW and reached wind speed between 6-12 m/s. Although this storm was not really severe, it did cause the breach of the dune on 18 January 2018.

The last storm occurred on 1 and 2 February 2018. This storm was similar to the previous storm. The offshore wave height was 2.0-3.2 m, the peak wave period was 6-11 s and the wave direction was NWW to N. At the sensor located most seaward the wave height was 1.7-2.0 m, the peak wave period was 8-12 s and the water depth was 2.9-3.1 m. At the sensor near mean sea level the wave height was 0.9-1.3 m, the peak wave period was 12-15 s and the water depth was 1.5-2.0 m. At the sensor located most landward the wave height was 0.7-0.8 m, the peak wave period was 15 s and the water depth was 0.7-1.0 m.

Although, 11 February 2018 was not classified as a storm surge, the water level did reach the sensor located at the upper part of beach.

2.4.2 Morphodynamics

It is interesting to see that the wave heights offshore were different for all storms, but that the wave heights in the subtidal zone were all more or less similar. Probably, the larger waves all

break over the ebb-tidal delta and the foreshore. Therefore, it seems especially the water level, which is related to the storm surge and the astronomical tide, determines how much erosion occurs because the water level determines how high the waves reach up at the dunes. The water levels during the storm surges were approximately 2 meters and erosion was especially seen above the NAP +2 m.

It is not possible to determine during which storms the erosion was largest. The first three storms were severe and probably resulted in a lot of erosion. At Ameland Northwest the dunes were still protected by the beach nourishment placed in 2015 (Fig. 2.14). The looser sand of the nourishment, which is easier to erode, and the non-natural slope of the beach probably resulted in larger erosion rates in this period. This made the beach more prone to erosion as water levels during less severe storms reached the most landward pressure sensor. This implicates that each storm reached the dunes. For example, the ninth storm was relatively calm but caused the dune to breach. Figure 2.14 and 2.15 show that the erosion took place at the foreshore, beach and dunes, but was most severe in the dune area. This is supported by the change in bed elevation at the pressure sensors which show most erosion at the most landward sensor. The alongshore current in front of the beach can easily transport the eroded sand, so more erosion can take place. The deposition more seaward is related to the onshore migration of the Bornrif. Where in previous years especially beach erosion occurred this storm season especially shows dune erosion. If no measures will be taken more dune breaches may occur in the future.

Table 2.4. Wind and wave data for all storm surges in the storm season of 2017/2018. The values for the pressure sensors are the values during high tide. The thick numbers represent the storm surges which exceeded the alarm level. n.d. = no data.

	Wind		Offshore			Sensor 55180			Sensor 55181			Sensor 55182		
Storm #	Wind speed (m/s)	θ (°)	H_s (m)	θ (°)	T_p (s)	H_{m0} (m)	T_p (s)	h (m)	H_{m0} (m)	T_p (s)	h (m)	H_{m0} (m)	T_p (s)	h (m)
1	10-21	230-270	2.7-6.4	250-290	4-11	n.d.	n.d.	n.d.	n.d.	n.d.	n.d.	n.d.	n.d.	n.d.
2	12-16	300-340	2.6-5.0	208-340	7-11	2.1-2.3	8-14	3.1-3.5	1.1- 1.3	14-15	1.5-2.4	0.6-0.7	16	0.6-0.9
3	**10-17**	**280-350**	**3.2-7.3**	**307-347**	**7-14**	**1.7-2.3**	**8-14**	**2.5-3.4**	**0.9-1.3**	**14-16**	**1.5-2.3**	**0.8**	**16**	**0.9**
4	6-13	260-310	2.2-5.0	285-325	6-11	1.9-2.0	7-13	2.6-3.1	0.9-1.2	14	1.5-2.0	0.6	16	0.6
5	6-12	290-330	3.1-5.5	298-342	8-12	n.d.	n.d.	n.d.	n.d.	n.d.	n.d.	n.d.	n.d.	n.d.
6	6-14	270-330	3.4-5.7	300-346	7-17	n.d.	n.d.	n.d.	n.d.	n.d.	n.d.	n.d.	n.d.	n.d.
7	6-12	80-200	1.8-3.0	316-360	13-14	n.d.	n.d.	n.d.	n.d.	n.d.	n.d.	n.d.	n.d.	n.d.
8	**10-22**	**240-280**	**1.8-6.0**	**257-329**	**4-12**	**1.6-2.2**	**4-14**	**3.0-3.5**	**1.0-1.5**	**13-16**	**1.5-2.3**	**0.8-1.1**	12	**0.7-1.2**
9	6-12	250-300	2.0-3.6	268-297	6-9	1.8-2.2	5-10	2.8-3.1	1.1-1.3	14-16	1.7-2.0	0.7-0.9	15-16	0.6-0.8
10	4-10	250-360	2.0-3.2	297-357	6-11	1.7-2.0	8-12	2.9-3.1	0.9-1.3	12-15	1.5-2.0	0.7-0.8	15	0.7-1.0

3 Part 2: Modelling the effect of the 2017/2018 storm season with XBeach

3.1 Introduction

To study the impact of storms on the coast of Ameland Northwest the morphological storm impact model XBeach was used (Roelvink et al., 2009). XBeach is a numerical model which simulates hydrodynamic and morphodynamic processes and their impact on the coast. The model was originally developed to model hurricane impacts on sandy beaches for the U.S. Corps of Engineers, but is now also applied to other types of coasts and purposes. In this research XBeach BETA release version 1.23 was used.

Near Ameland Northwest the bathymetry is complex because of the ebb-tidal delta of the Ameland tidal inlet. The water depth on the ebb tidal delta is relatively low and causes wave breaking of the larger waves. Therefore, only limited wave energy will eventually reach the beach. The performance of XBeach for this complex bathymetry was validated with measurements for the 2017/2018 storm season.

3.2 Methods

3.2.1 Model set-up

To validate the hydrodynamics and morphodynamics, the transect which is used as input for the model is based on the locations of the three pressure sensors on the beach and extended to approximately -20 m offshore (Fig. 3.1A). The bed elevation along this transect is composed by using different available datasets and should resemble the situation as it was at the start of the measuring period of the pressure sensors. Most offshore, the transect is composed of 'vaklodingen'. At the beach the transect measured with RTK-GPS on the day of pressure sensor installation (21 September 2017) is used. The first dune row consists of LiDAR bed elevation data obtained on 22 September 2017**.** The dune area more landward is composed of AHN (Algemeen Hoogtebestand Nederland) data. The set-up of the data is shown in Table 3.1. It is especially important that the bed elevations of the beach and first dune row are collected in the same period the measurements began. It should be noted that the bed elevations of the 'vaklodingen' do not fit to the bed elevations of the measured transect. The bed elevations of the nearshore were measured earlier in 2017, and because the morphological system is dynamic the bed elevations have likely changed. This must be kept in mind when comparing model computations with the measurements. To connect these two bed elevation datasets the bed elevation were linearly interpolated over 5 m. The cross-shore grid size of the model varies between 5 m offshore to 1 m onshore (Fig. 3.1C).

At the offshore boundary of the transect, wave characteristics (significant wave height H_{m0}, wave peak period T_p, angle of wave incidence θ, directional spreading coefficient (s), and water levels η are imposed (Fig. 3.3). The wave characteristics are based on wave buoy Amelander Zeegat 1_1 and if not available on wave buoy Amelander Zeegat 1_2 (Fig. 2.2). The water levels are based on wave buoy Wierumergronden. The wave characteristics and water levels vary over time. The wave characteristics are determined for each hour and the water levels for each half an hour. Modelling the whole storm season of 2017/2018 is very time consuming. Therefore, only the periods which are considered as important for dune erosion are modelled. In total twelve periods are selected based on a wave height higher than 2.5 m (Fig. 3.2). These storm periods should be in the measuring period of the pressure sensor because the initial profile mimics the situation at the start of the measuring period. For

the last part of the measuring period no wave data is available. However, based on Figure 2.7 it is assumed only one big storm occurred in this period. The output bed profile of each storm period is used as input bed profile for the next storm period. This way there are no sudden jumps in water level.

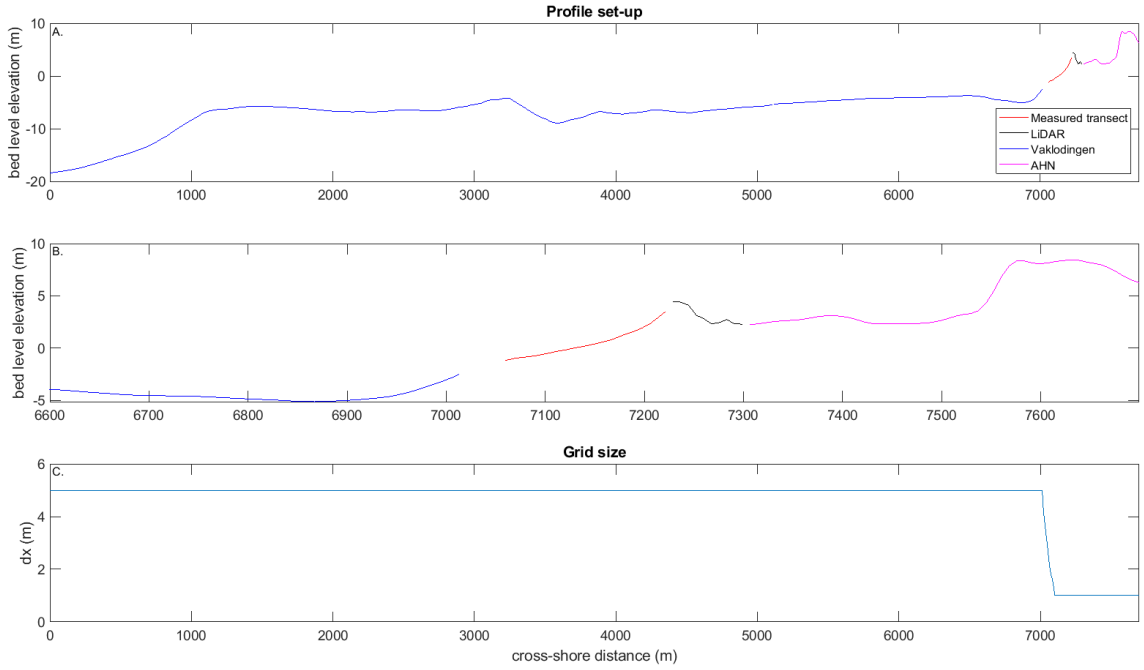

Table 3.1. Data sources for initial XBeach profile.

Data source	Resolution	Date
Vaklodingen	20 x 20 m	2017
GPS measurements transect	<1 m	21 September 2017
LiDAR	2 x 2 m	22 September 2017
AHN	5 x 5 m	2017

As breaking formulation ‘Roelvink2’ is used (Roelvink, 1993). The breaking parameter gamma is set to 0.45 instead of the default value of 0.55, because this gave better results for profiles with a gentle foreshore (Hoonhout & Van Thiel de Vries (2012); Wesselman et al. (2018)). A morphological acceleration factor (morfac) of 1 is applied because the modelled hydrodynamics are compared to the measured hydrodynamics. All other parameters are set to their default values (Deltares, 2015). No alongshore current is modelled because a 1-D model is used. However, the alongshore current probably plays a role in the removal of deposited sediment on the foreshore. Therefore, also a scenario is modelled where the deposition on the foreshore is manually removed between each modelled period.

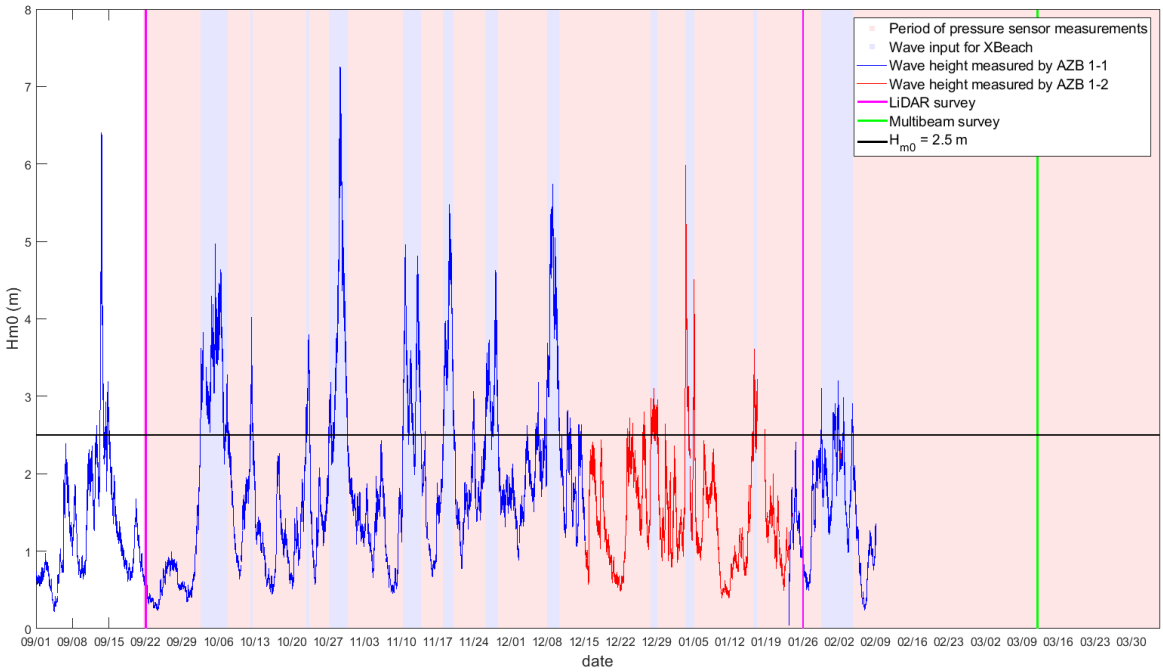

Figure 3.2. Wave height at the wave buoy Amelander Zeegat 1_1 (red line). When no wave data was available the wave height at Amelander Zeegat 1_2 was used (blue line). The red box indicates the measuring period of the pressure sensors. The blue box indicates the periods used as input for the XBeach model. The purple lines show the moment when the LiDAR surveys were conducted and the green lines shows the moment when the multibeam survey was conducted. The black line indicates H_{m0} = 2.5 m.

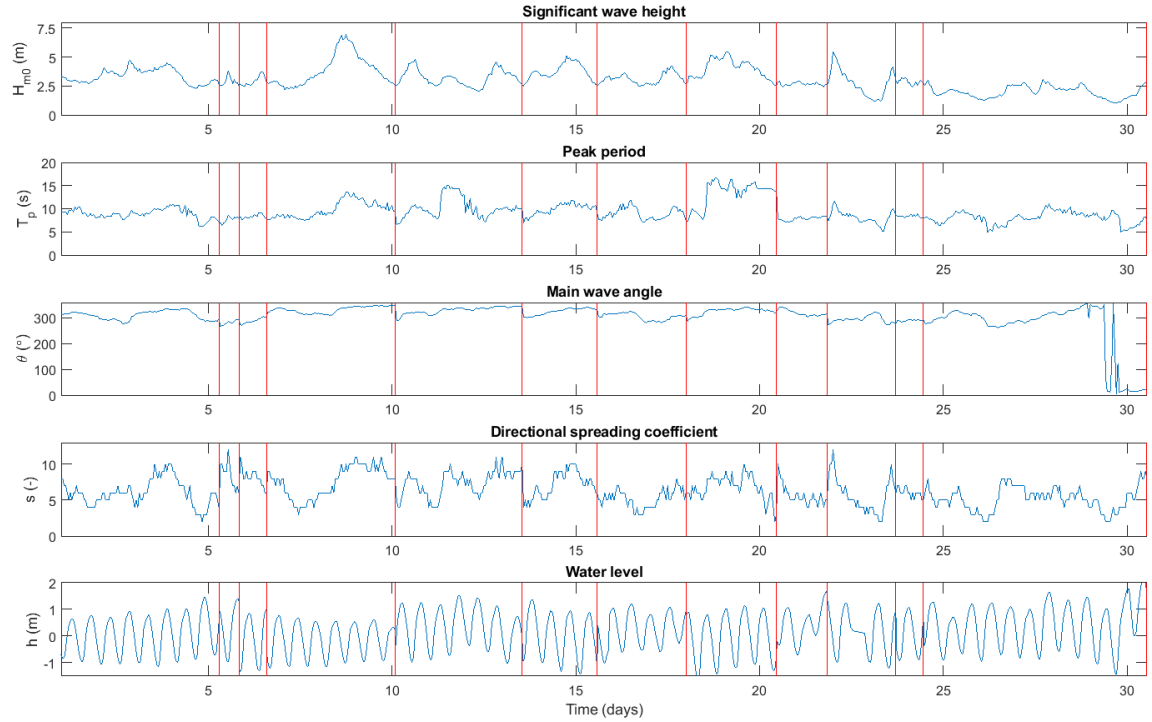

Figure 3.3. Time series of boundary conditions during the selected periods during the storm season of 2017/2018 used in XBeach. The red lines are the boundaries between the periods. From top to bottom: significant wave height H_{m0} (m), wave peak period T_p (s), mean wave angle θ (°), directional spreading coefficient s (-) and water level h (m).

3.2.2 Extracting significant wave height for low and high frequency waves

3.2.2.1 Pressure sensor data

From the sea surface elevation collected with the pressure sensors the wave spectrum can be determined with:

$$E(f) = \lim_{\Delta f \to 0} \frac{1}{\Delta f} E\{\frac{1}{2}\underline{a}^2\} \tag{3.1}$$

where Δf is the frequency interval, and $E\{\frac{1}{2}\underline{a}^2\}$ is the variance with *a* as sea surface elevation. The pressure sensors collected data with a frequency of 6 Hz and the wave spectrum was determined for every 20 minutes. To determine the significant wave height H_{m0} of the low frequency (infragravity waves) and high frequency (sea and wind waves) waves, the spectral moment was determined:

$$m_0 = \int_{f1}^{f2} E(f) df \tag{3.2}$$

where *f* is the wave frequency, and *E(f)* is the variance density spectrum. The low frequency range is determined as f_1 = 0.005 Hz and f_2 = 0.05 Hz, and the high frequency range as f_1 = 0.05 Hz and $f_2 = f_n$ which is the Nyquist frequency and is defined as:

$$f_n = \frac{1}{2\Delta t} \tag{3.3}$$

where Δt is the sampling interval of the wave record. From the spectral moment the spectral wave height can be determined with:

$$H_{m0} = 4\sqrt{m_0} \tag{3.4}$$

3.2.2.2 XBeach output

For this study the 'surfbeat' mode is used. This means short wave variations and associated long waves are resolved on the wave group scale. To determine the significant wave height computed by the XBeach model the output H, Hrms wave height based on instantaneous wave energy, and *zs*, water level, are used. The method used to determine the significant wave height from the sea surface elevation measurements is also used to determine the significant wave height for XBeach model results (eq. 3.1, 3.2 & 3.4) where the sea surface elevation is *zs*. However, this is only a part of the high frequency wave spectrum ($H_{mo,HF,1}$). The second part of the $H_{m0,HF,2}$ can be determined from the H_{rms}. H_{rms} is related to H_{mo} by:

$$H_{mo,HF,2} \approx \sqrt{2} * \sqrt{\frac{1}{N}\sum_{n=1}^{N} {H_{rms}}^2} \tag{3.5}$$

where *N* is the number of data points and H_{rms} is the root mean square wave height. The total $H_{m0,HF}$ can be determined by:

$$H_{m0,HF} = \sqrt{{H_{m0,HF,1}}^2 + {H_{m0,HF,2}}^2} \tag{3.6}$$

3.2.3 Effect profile changes on wave parameters pressure sensors

At the start and end of the measurement period of the pressure sensors the bed elevation was measured (Table 2.3). Beneath all sensors severe erosion occurred. When converting the pressure data into sea surface elevations, this change in bed level is not included. To determine the impact of this change the H_{m0} is determined for the bed level at the start and for the bed level at the end of the measuring period. Figure 3.4, 3.5 and 3.6 show the differences in H_{m0} and in Table 3.2 the mean and standard deviation of H_{m0} for the low and high frequency waves are shown.

Table 3.2.Mean and standard deviation of the significant wave height H_{m0} for low and high frequency waves determined with the bed level before and after the measurement period for pressure sensors 055180, 055181 and 055182.

		Sensor 055180		Sensor 055181		Sensor 055182	
		Initial bed level	Final bed level	Initial bed level	Final bed level	Initial bed level	Final bed level
High frequency waves	Mean H_{m0} (m)	0.76	0.80	0.58	0.61	0.50	0.52
	Standard deviation H_{m0} (m)	0.43	0.46	0.23	0.25	0.27	0.29
Low frequency waves	Mean H_{m0} (m)	0.14	0.13	0.14	0.14	0.27	0.27
	Standard deviation H_{m0}	0.11	0.11	0.11	0.11	0.17	0.17

The differences in H_{m0} are small for all sensors (0.01-0.04 m). Therefore, the initial bed level is used for the validation of XBeach and no bed level adjustments are made over time.

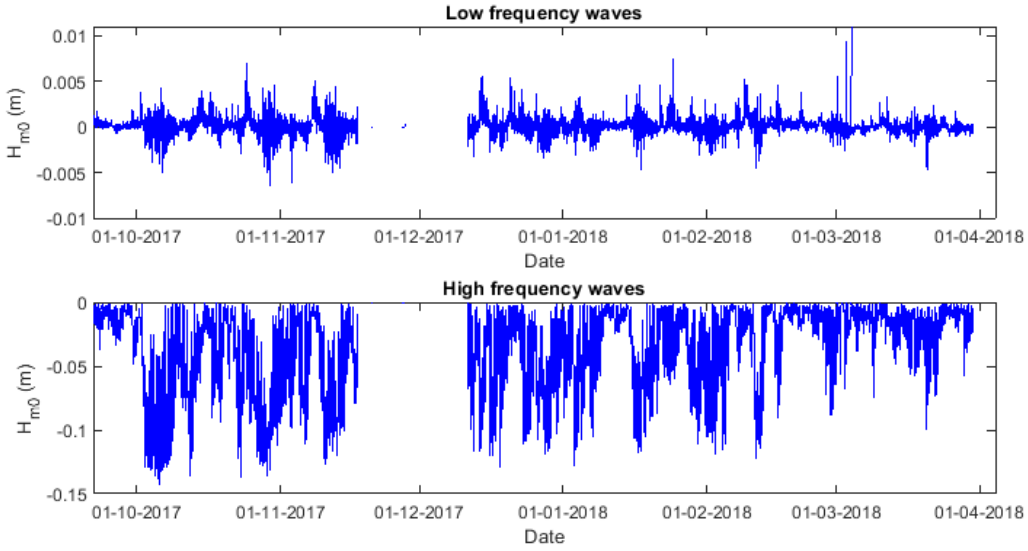

Figure 3.4. Difference between significant wave heights determined with the bed level at the start (-1.39 m NAP) and end (-2.15 m NAP) of the measurement period for pressure sensor 055180. A negative value means the wave height determined with the bed level at the start of the measurement period was smaller than the wave height determined with the bed level at the end of the measurement period.

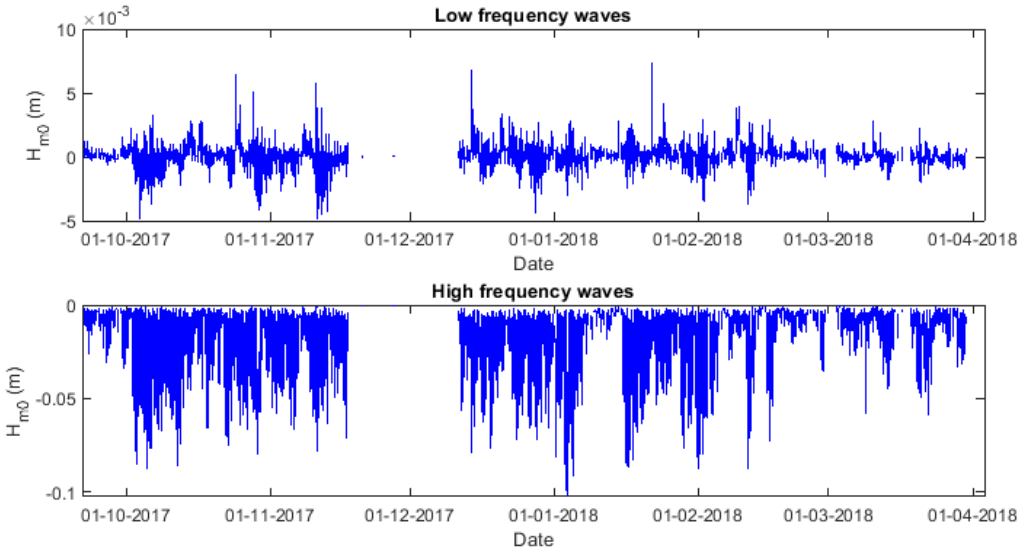

Figure 3.5. Difference between significant wave heights determined with the bed level at the start (-0.18 m NAP) and end (-0.90 m NAP) of the measurement period for pressure sensor 055181. A negative value means the wave height determined with the bed level at the start of the measurement period was smaller than the wave height determined with the bed level at the end of the measurement period.

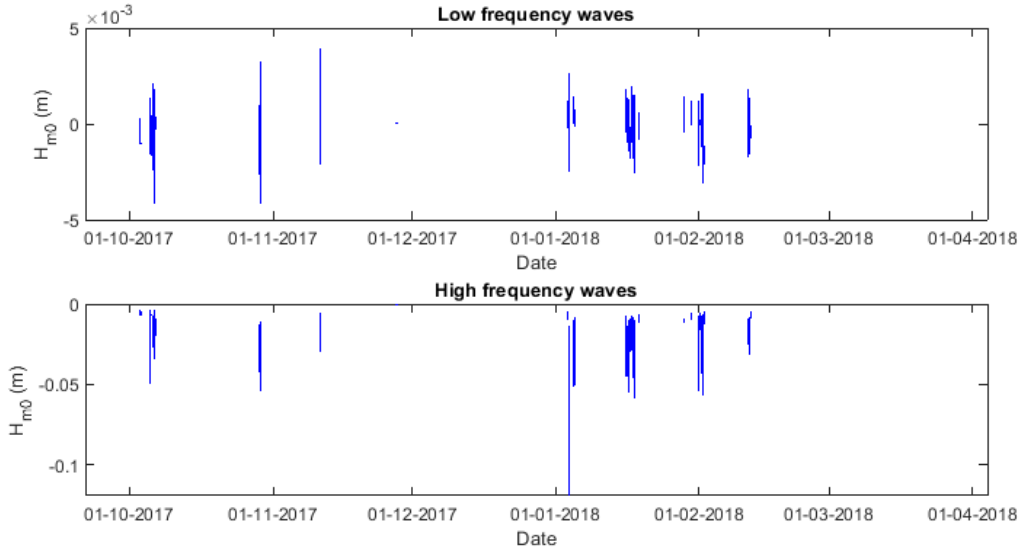

Figure 3.6. Difference between significant wave heights determined with the bed level at the start (1.40 m NAP) and end (0.27 m NAP) of the measurement period for pressure sensor 055182. A negative value means the wave height determined with the bed level at the start of the measurement period was smaller than the wave height determined with the bed level at the end of the measurement period.

3.3 Results & discussion

3.3.1 Validation hydrodynamics

To determine which scenario (with or without foreshore removal) is most reliable, the model results are validated against the measured H_{m0} of the pressure sensors (Table 3.3). There are barely any differences in the r^2 and also for the modelled low frequency waves the bias is similar. However, there are differences in the modelled high frequency waves. Especially, later in the simulation the differences become larger because of larger deviations of the bed levels. The differences of both modelled scenarios with the measured wave heights are shown in Appendix A. At the most seaward and the most landward pressure sensor the scenario with foreshore removal shows a lower bias (-0.035 m and -0.126 m versus -0.121 m and -0.156 m, respectively) while at the middle sensor the scenario without foreshore removal shows a lower bias (0.047 m versus -0.001 m) (Table 3.3). The modelled erosion is also more realistic for the scenario with foreshore removal. This will be discussed in section 3.4. Because the scenario with foreshore removal yields better results for the hydrodynamics, only this scenario is discussed further.

Figure 3.7, 3.8 and 3.9 show the significant wave height of the low and high frequency waves modelled by XBeach and the measured wave heights for the three pressure sensors. The scatter plots of the measured and modelled wave heights for all pressure sensors are shown in Figure 3.10. Observed low-frequency wave height ranges between 0.1 and 0.8 m at the lowest sensor, between 0.1 and 0.7 at the middle sensor and between 0.1 and 0.6 m at the highest sensor.

The computed low-frequency waves reasonably agree with the measurements at the lowest sensor. The model tends to overestimate the low-frequency waves by 0.1-0.2 m at the middle sensor. At the highest sensor, the model underestimates the low-frequency wave heights by about 0.1 in the first four storms and overestimates the low-frequency wave by about 0.1 m in the last storms. Sometimes, when the measured low frequency waves decreases with ~0.1

m, the modelled low frequency waves show an increase of 0.1-0.2 m. This may due to the fact that the breaking point of the short waves is located seaward of the middle sensor but is modelled landward.

XBeach generally underestimates the high frequency waves at the lowest sensor by a few decimetres, although in periods 5 and 12 the computed wave heights show reasonable agreement with the measurements. Peaks in low frequency wave height correspond with peaks in high frequency wave height. During wave breaking, energy is transferred from higher frequencies to lower frequencies. Higher high frequency waves will therefore result in higher low frequency waves.

The high-frequency waves are sometimes underestimated and sometimes overestimated by about 0.1-0.2 m at the middle sensor. Gaps in the measured data do not necessarily mean that the water did not reach the cross-shore location of the pressure sensor. The pressure sensor only measured waves when the water level was high enough to reach the elevation of the pressure sensor.

At the highest sensor, water levels were not always high enough to reach the sensor. Between the second and third pressure sensor the modelled low frequency wave height decreased most of the time because of breaking waves. The low frequency waves show a clear dependency on the tide.

In the scatter plots in Fig. 3.10 it can be seen that the correlation can be different for the different storm periods. At sensors 055180 and 055181 the low frequency waves show similar correlations, whereas at sensor 055182 the early storm periods show underestimation with a poor correlation and storm periods 11 and 12 a small overestimation with reasonably fair correlation. This can be related to the lower offshore wave heights used as boundary conditions (Table 3.4). These waves are less influenced by the complex ebb tidal delta bathymetry. Period 11 shows also a deviation from the other periods for the high frequency waves. At all sensors the high frequency wave height seems underestimated. This could be related to the relatively low water levels used as input for this storm period.

Wesselman et al. (2018) also validated a 1-D XBeach model against measured waves collected with pressure sensors at Schiermonnikoog. Their r^2's were much higher for the high frequency waves (0.86-0.92), and also for the low frequency waves reached above the 0.80. The less good agreement found here is likely due to a more complex 2D bathymetry at Ameland NW and large uncertainties in morphological development.

The complex bathymetry of the Ameland ebb tidal delta is likely not captured sufficiently in a 1D XBeach model. Where in the model all waves with different angles are forced over a cross-shore transect, in reality the waves will follow different paths over a 2D ebb tidal delta bathymetry. Moreover, as limited data was available of the nearshore morphological changes during the storm season, uncertainties about the profile used as an input to the model are relatively large.

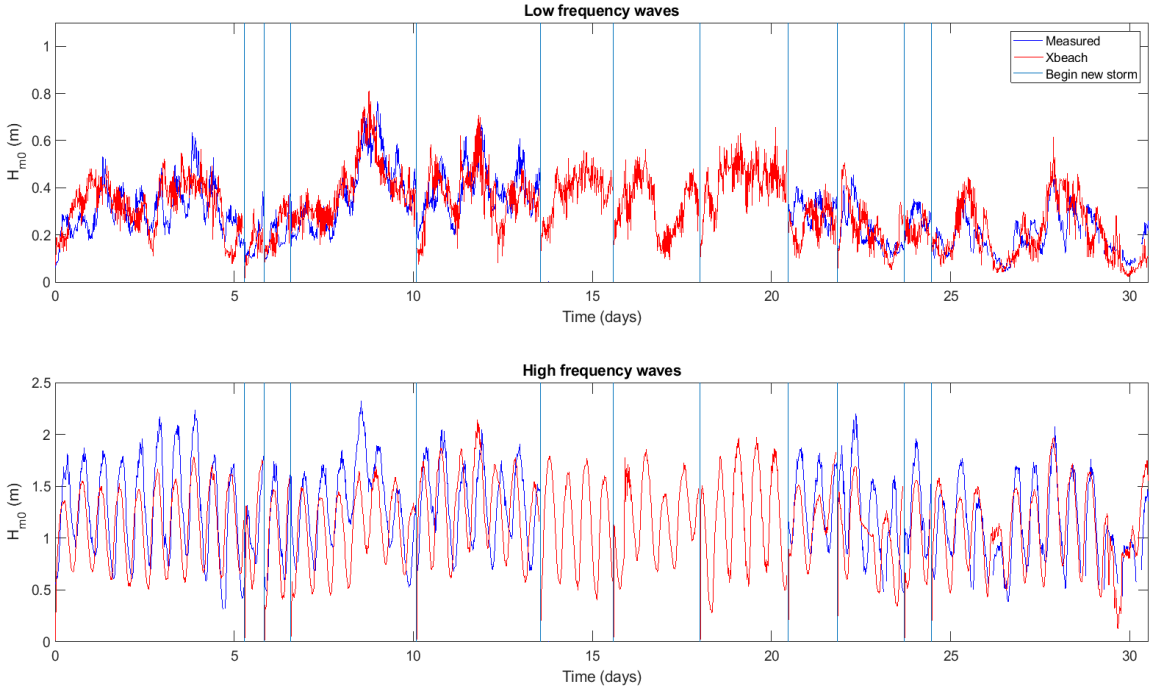
Low frequency waves
Measured
Xbeach
Begin new storm
H_m0 (m)
Time (days)
High frequency waves
H_m0 (m)
Time (days)

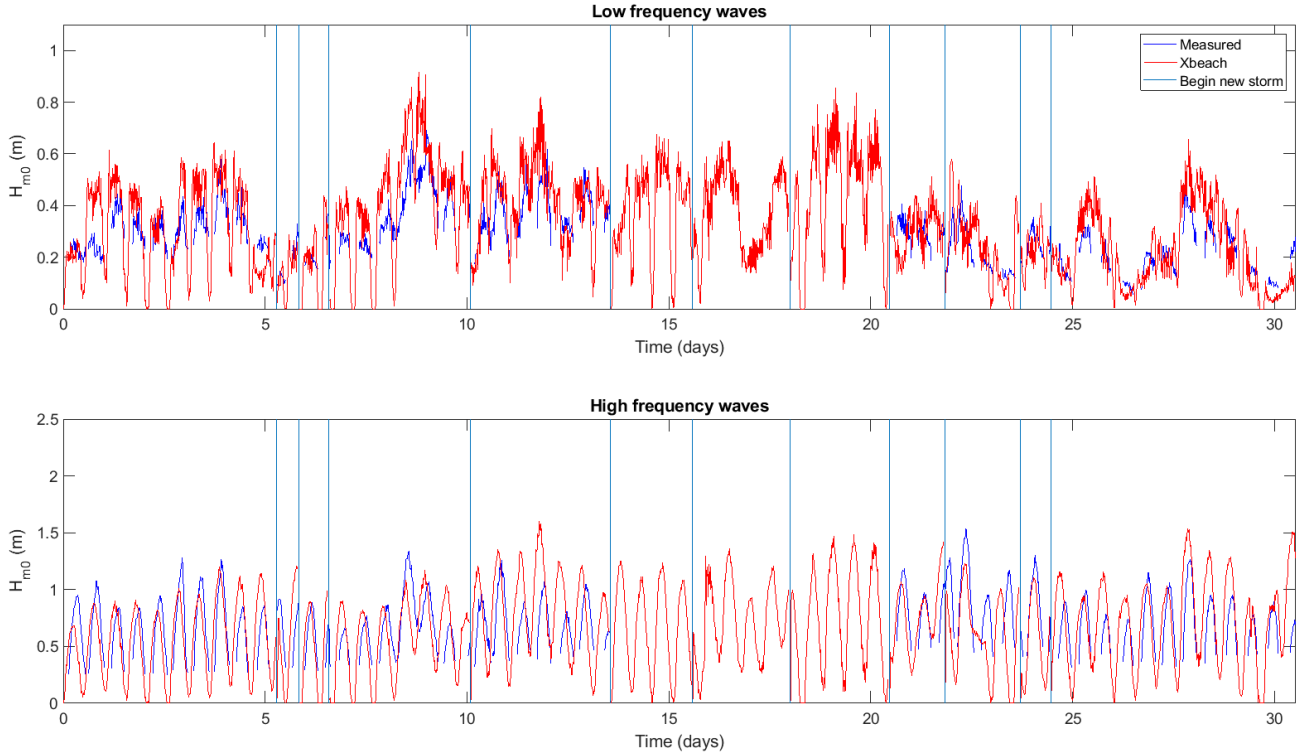

Figure 3.8. Measured (blue) and computed (red) significant wave height H_{m0} for low and high frequency waves at pressure sensor 055181. The vertical lines indicate the different storm periods.

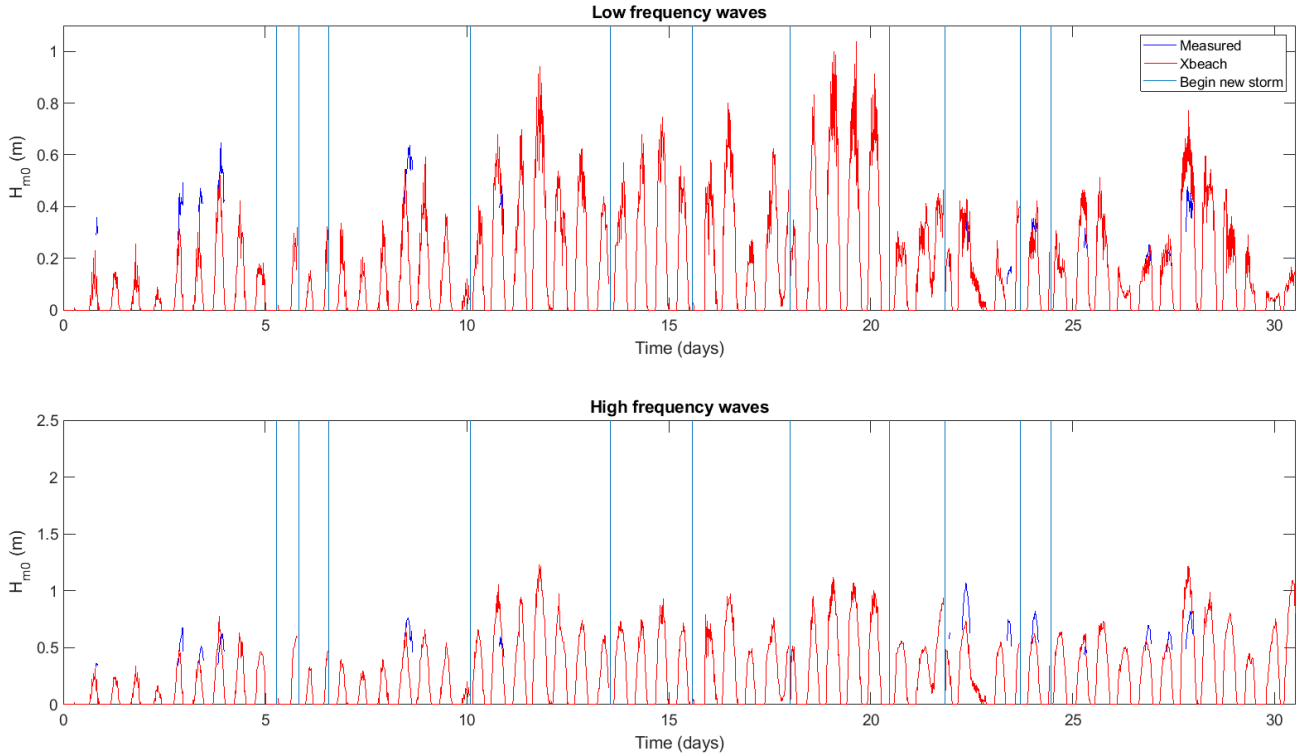

Figure 3.9. Measured (blue) and computed (red) significant wave height H_{m0} for low and high frequency waves at pressure sensor 055182. The vertical lines indicate the different storm periods.

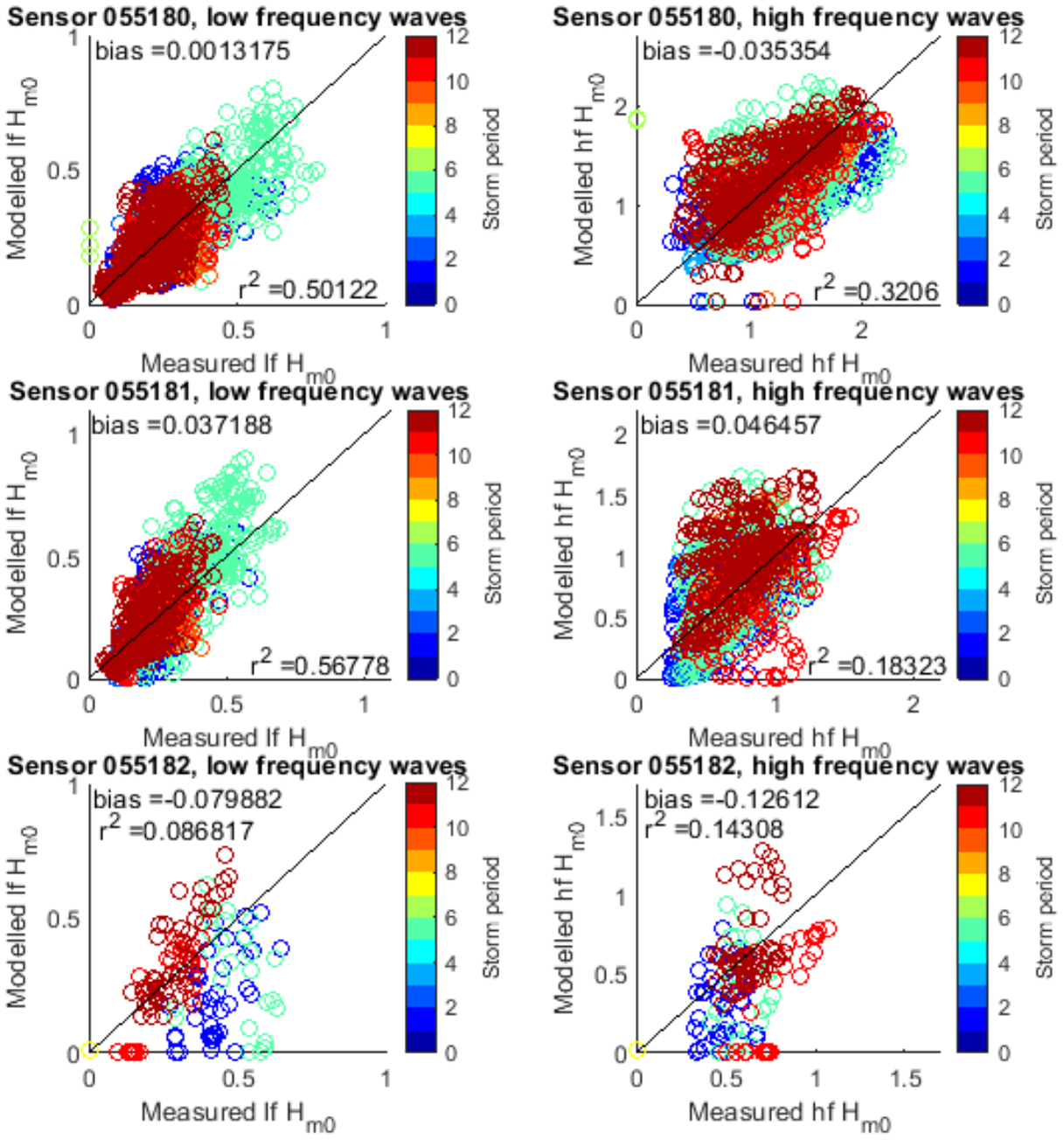

Figure 3.10. Measured versus modelled low frequency H_{m0} (left panels) and high frequency H_{m0} (right panels) for pressure sensors 055180 (upper panels), 055181 (middle panels) and 055182 (bottom panels). The black lines indicate the 1:1 position. The colours indicate storm period.

3.3.2 Validation morphodynamics

The modelled and measured bed level changes are shown in Figure 3.11. The measured bed level is composed of the multibeam survey conducted on 12 March 2018, the LiDAR survey conducted on 26 January 2018 and the bed level near the pressure sensors measured on 4 April 2018. It should be noted that the LiDAR survey was conducted between storm event 11 and 12.

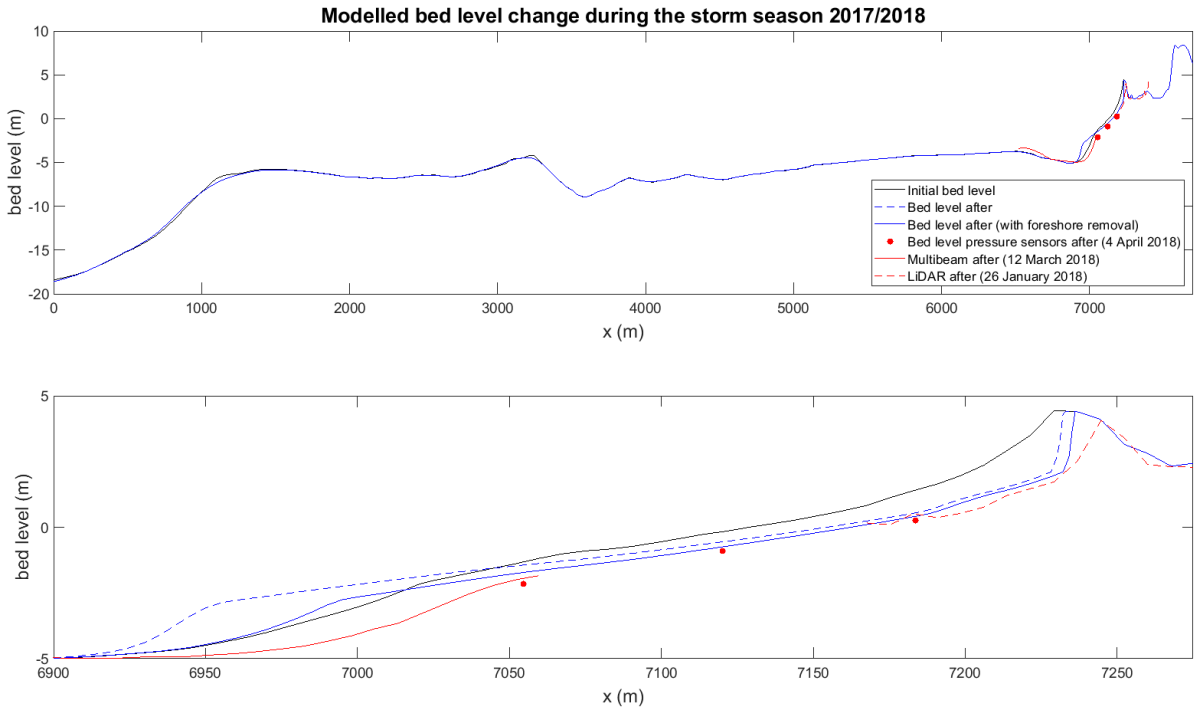

Figure 3.11. Modelled and measured bed level elevations. The blue lines are the model results (solid is with foreshore removal and dashed is without foreshore removal), the red lines and dots are the measured elevations and the black line is the initial profile. Note that the LiDAR survey is conducted between storm period 11 and 12.

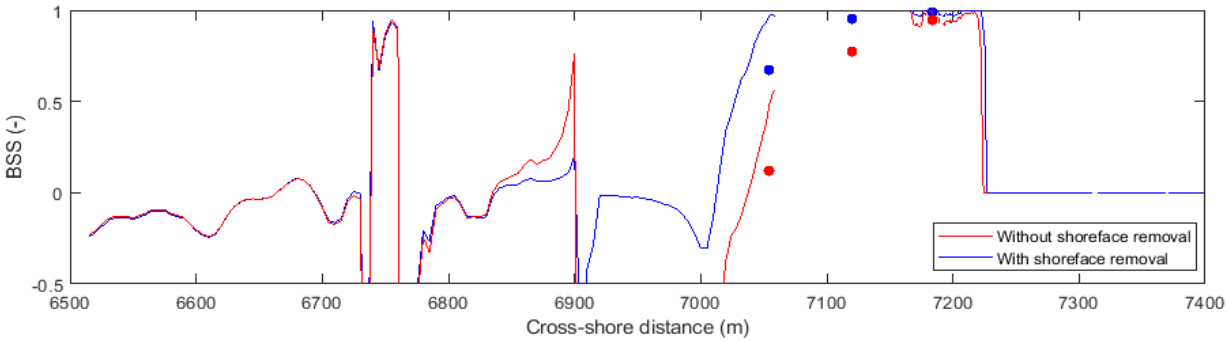

Figure 3.12.BSS of the XBeach simulation compared with the measurements. The dots indicate the pressure sensors and the lines the LiDAR (dunes) and multibeam (foreshore) survey.

The bed level changes computed with the model shows sedimentation on the foreshore. The measurements show erosion here. This is likely caused by a strong alongshore current that is not included in the 1D model. Also, only storm conditions were computed with the model and not the calmer conditions with lower water levels during which the sedimentation may have been removed from the profile. To mimic these effects, the foreshore was manually removed between each storm period. This results in less wave breaking on the foreshore and therefore

more erosion higher up on the beach and at the dunes (Fig 3.11 & Table 3.6), which is more in line with the measurements. However, the erosion of the foreshore is not captured by the 1D model.

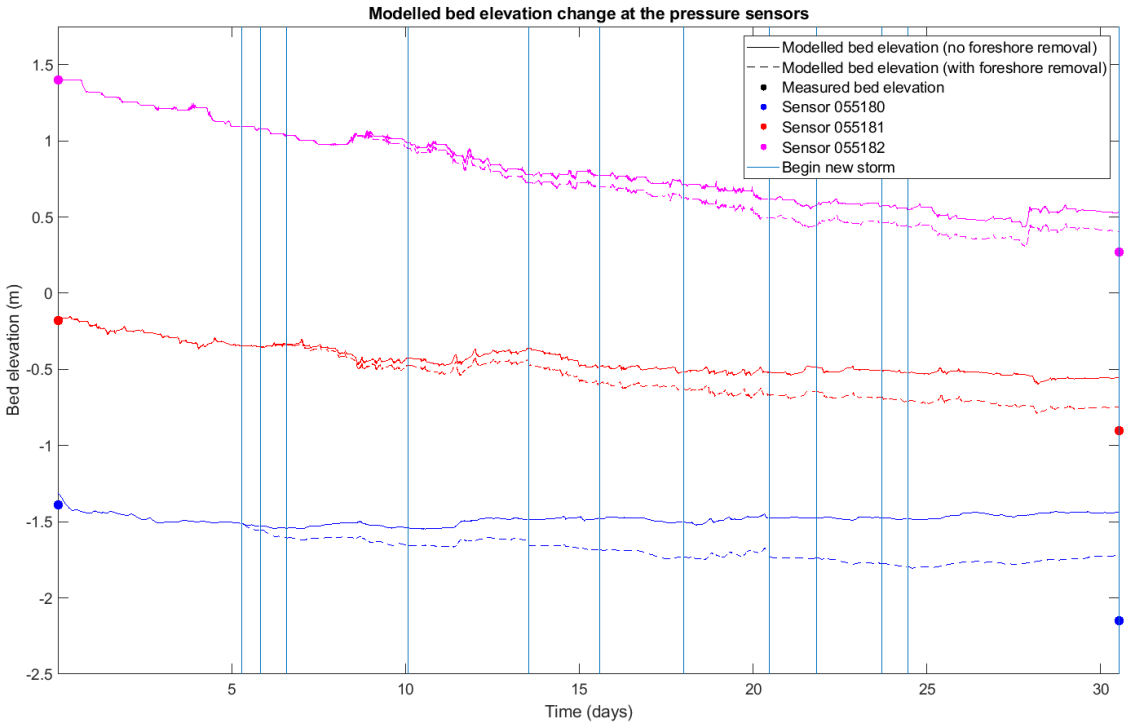

Figure 3.13. Modelled bed elevation change at pressure sensors 055180 (blue), 055181 (red) and 055182 (magenta). The dots are the measured initial bed elevations at the sensors and the measured final bed elevations at the sensors. The dashed lines are the modelled bed levels with foreshore removal and the solid lines are the modelled bed levels without foreshore removal.

The measurements shows erosion over the entire profile, tens of meters shoreward. The model underestimates this erosion. Figure 3.12 shows the BSS of the modelled bed elevation per grid cell. According to the BSS classification of Van Rijn et al. (2003) the morphological reproduction was excellent for the upper part of the beach up to the final modelled dune foot. For the scenario with foreshore removal the most seaward pressure sensor 055180 has a good BSS (0.68) and pressure sensors 055181 and 055182 have excellent BSSs (0.95 and 0.99, respectively). This is a considerable improvement compared to the scenario without foreshore removal where the BSSs were 0.12, 0.77 and 0.94, respectively. The same can be seen in Figure 3.13 which shows the modelled bed elevation change at the pressure sensors. The bed level change for the scenario with foreshore removal at pressure sensor 055180, 055181 and 055182 is -0.76 m, -0.72 m and -1.13 m, respectively. The modelled bed level change is -0.12 m, -0.39 m and -0.86 m, respectively. Landward of the dunes aeolian processes drive sand transport. These processes are not modelled and therefore no bed level

change are computed which results in a BSS of 0. At the location of the most seaward pressure sensor the modelled bed elevation corresponds well with the multibeam bed elevation. However, the BSS quickly decreases offshore to even negative values. Negative values mean that instead of erosion, deposition occurs or vice versa. The onshore migration of the Bornrif is seen in the measured bed elevation, but is not modelled. This difference is likely due to the fact that this migration is driven more by daily conditions and less by storm conditions (Nederhoff et al., 2016).

3.3.3 Modelled development Ameland Northwest

Table 3.6 shows the volume change for each storm event and Figure 3.14 shows the bed level change for each storm event separately. The volume change is calculated for the area above -1.39 m which is the initial bed level of the most seaward pressure sensor. Also, the volume change is calculated above 2 m because this represents the dune foot and so the dune erosion can be determined. The total volume change for the scenario without foreshore removal is -144.3 m^3/m for the whole area and -47.2 m^3/m at the dunes. The scenario with foreshore removal showed more erosion (-155.5 m^3/m and -60.3 m^3/m, respectively). Only the scenario with foreshore removal is discussed, because this scenario is assumed to be more realistic. During the first storm event the beach is severely eroded (-30.7 m^3/m) with little dune erosion (-0.7 m^3/m). The second and third storm periods are short and show some beach erosion (-3.0 and -2.2 m^3/m, respectively), but barely any dune erosion (-0.4 and 0 m^3/m, respectively). During the fourth period the waves are highest (Table 3.4) but the water level is relatively low. Therefore, the waves are not able to reach the dunes and this explains the high erosion rates on the beach and small effects on the dunes. The fifth period is the first period where considerable dune erosion occurred (-15.7 m^3/m). Compared to the previous periods the water levels are relatively high (Table 3.4) and therefore the waves are able to erode the dunes. Also, the beach erosion of the previous storms makes the dunes more prone to erosion. This storm period is very comparable to the first storm period, but results in a different erosion patterns (Table 3.4). During the sixth and seventh storm period the erosion mainly takes place on the beach. The eighth storm period has relatively low water levels but still considerable dune erosion occurs during this period. This may be explained by the high wave heights and wave peak periods for this storm (Table 3.4). In storm period 9 the water level is relatively high, but the wave height is relatively low. This combination leads to moderate erosion of the dunes (-3.0 m^3/m) which is relatively high for this short period. In storm period 10 the water levels are lower and the wave heights are higher again. This results in relatively more beach erosion. Storm period 11 is short and the low waves and water level results in low erosion rates (-2.8 m^3/m). The last storm period is the longest. During this period the wave height is relatively low, but the water levels are relatively high. Although the dune erosion per day is moderate (-3.0 m^3/m), this event results in high dune erosion (-18.4 m^3/m) because of the long storm period. Summarizing, only storm periods 4, 8 and 12 caused the dune erosion, but this only occurs because previous storms eroded the beach.

Table 3.6. Volume change per storm event above z = -1.39 m (initial bed elevation at pressure sensors 055180) and above z = 2 m. Because all storm events have different durations the volume change per day is shown between brackets. This gives an indication about the relative erosion.

Volume change (m^3/m)	Storm event 1	Storm event 2	Storm event 3	Storm event 4	Storm event 5	Storm event 6	Storm event 7	Storm event 8	Storm event 9	Storm event 10	Storm event 11	Storm event 12	**Total**
> -1.39 m (no foreshore removal)	-30.7 (5.8)	-2.3 (-4.3)	-2.2 (-3.0)	-11.0 (-3.2)	-15.7 (-4.6)	-7.8 (-3.9)	-7.3 (-3.1)	-13.3 (-5.4)	-2.6 (-1.9)	-3.8 (-2.0)	-1.5 (-2.1)	-16.2 (-2.7)	**-114.3**
> 2 m (no foreshore removal)	-0.7 (-0.1)	-0.4 (-0.8)	0 (0)	-0.8 (-0.2)	-13.7 (-4.0)	-1.1 (-0.5)	-2.1 (-0.9)	-8.2 (-3.4)	-2.5 (-1.8)	-2.2 (-1.2)	-0.7 (-0.9)	-15.0 (-2.5)	**-47.2**
> -1.39 m (with foreshore removal)	-30.7 (-5.8)	-3.0 (-5.8)	-3.5 (-4.8)	-17.1 (-4.9)	-21.2 (-6.2)	-14.1 (-7.0)	-10.8 (-4.5)	-20.4 (-8.4)	-4.8 (-3.5)	-6.7 (-3.6)	-2.8 (-3.9)	-20.3 (-3.4)	**-155.5**
> 2 m (with foreshore removal)	-0.7 (-0.1)	-0.4 (-0.8)	0 (0)	-0.9 (-0.3)	-15.7 (-4.6)	-1.7 (-0.8)	-3.0 (-1.3)	-12.4 (-5.1)	-3.0 (-2.2)	-3.2 (-1.7)	-0.8 (-1.1)	-18.4 (-3.0)	**-60.3**

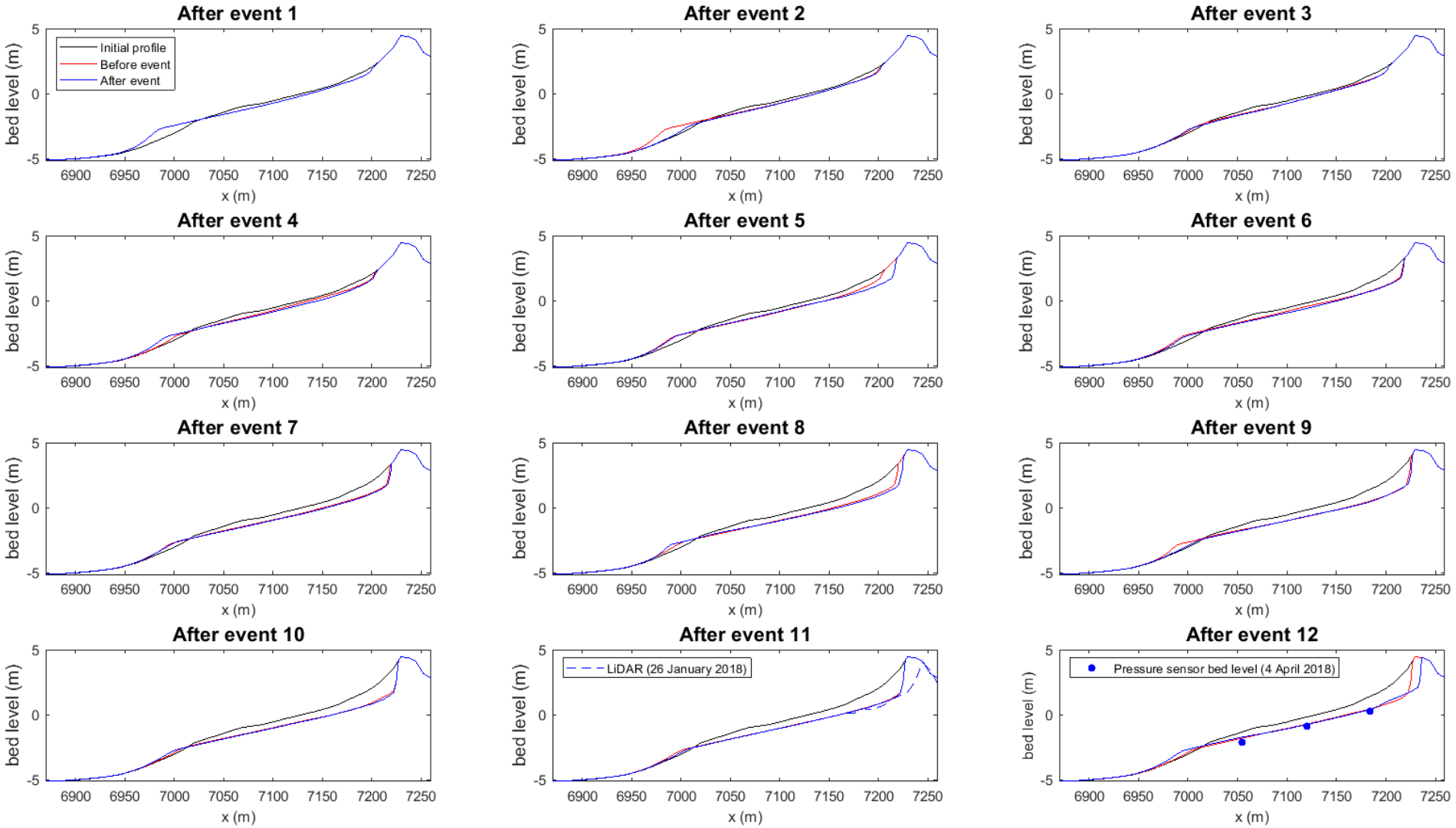

Figure 3.14. The bed elevation change per storm event for the scenario where the foreshore is manually removed after each event. The black line is the initial profile, the red line is the profile before the event and the blue line is the profile after the event. The LiDAR survey is shown after event 11 because the LiDAR survey was conducted between event 11 and 12.

4 Conclusions and recommendations

4.1 Conclusions

This report describes the effect of storm season 2017/2018 on waves and morphology at Ameland Northwest. Over the last tens of years the beach of Ameland Northwest shows an eroding trend. The QRF performed wave measurements with pressure sensors on the beach during the entire storm season. LiDAR bed level measurements were made before and after the storm season. These measurements were used to validate a 1D-XBeach simulation of beach and dune behaviour.

Compared to previous years this storm season was relatively strong. A total of 10 storm surges occurred of which two storms exceeded the alarm level. Two storm reached wind force 9 and four storms reached wind force 7. The high wind speeds were mostly directed from the W/NW. North of the ebb tidal delta the wave height corresponding to the storms was mostly higher than 4 m. Only the last two storm surges show wave heights around 2 m. The highest wave height measured was 7.4 m. Wave heights measured during these storm events at the most seaward located pressure sensor on the beach varied between 2-2.5 m. This is caused by the relatively shallow ebb-tidal delta which causes breaking of the larger waves. While the offshore water level was not necessarily higher during the storm events, this was the case at the beach. At the most seaward sensor water depths reached up to 3 m which was 0.5-1.0 m higher than during calm conditions. At the pressure sensor located at mean sea level the wave height was larger than 1 m and the water depth was about 2 m. The wave peak period increased here to 10-15 s. The most landward located sensor (above mean high water) measured only during strong storm surges. The wave heights varied here between 0.5 and 1.0 m, the peak period was about 15 s and the water level was approximately 0.9 m. The storm events caused erosion of the foreshore and the beach. Most erosion took place above NAP +2 m. A dune breach occurred on 18 January 2018.

The computed low-frequency waves reasonably agreed with the measurements at the lowest sensor (mean low water). The model tended to overestimate the low-frequency waves by 0.1-0.2 m at the middle sensor (mean sea level). At the highest sensor (just above mean high water), the model underestimated the low-frequency wave heights by about 0.1 in the first four storms and overestimates the low-frequency wave by about 0.1 m in the last storms. Sometimes, when the measured low frequency waves decreased with ~0.1 m, the modelled low frequency waves showed an increase of 0.1-0.2 m. This may due to the fact that the breaking point of the short waves was located seaward of the middle sensor but modelled landward.

XBeach generally underestimated the high frequency waves at the lowest sensor by a few decimetres. The high-frequency waves were sometimes underestimated and sometimes overestimated by about 0.1-0.2 m at the middle sensor. The pressure sensor only measured waves when the water level was high enough to reach the elevation of the pressure sensor. At the highest sensor, water levels were not always high enough to reach the sensor. Between the middle and highest pressure sensor the modelled low frequency wave height decreased most of the time because of breaking waves. The low frequency waves showed a clear dependency on the tide.

The XBeach morphodynamics showed good agreement with observed bed level changes in the upper part of the beach profile and the seaward side of the dune. The model was not able to model the erosion of the foreshore. This is likely caused by a strong alongshore current, which is a 2D effect that is not captured in the 1D model. Also, only storm conditions were computed with the model and not the calmer conditions with lower water levels during which the sedimentation may have been removed from the profile. To mimic these effects, the foreshore was manually removed between each storm period. This resulted in less wave breaking on the foreshore and

therefore more erosion higher up on the beach and at the dunes which was more in line with the measurements.

Three out of the ten storm caused dune erosion, but this only occurred because previous storms eroded the beach.

4.2 Recommendations

Modelling

To improve the model several steps can be taken. Firstly, the model can be extended to a 2D model. In a 1D model all waves will follow the same transect, but actually all waves will follow a different path over the ebb tidal delta toward the coast, because of differences in wave characteristics (wave height, wave angle, etc.). By making the model 2D the wave dissipation over the Bornrif will be modelled more accurately. Also, in a 2D model an alongshore current is present which is important in the erosion of the foreshore. Modelling of an entire storm season in XBeach is time consuming. We recommend focussing more on one storm when modelling in 2D. This also requires field data on shorter time scales (days).

We would recommend linking up QRF more with long-term projects so that 'fast follow-up studies' have a broader basis and can therefore actually be implemented 'quick'.

Models for beach and dune erosion at the study site were not ready-to-use, so that these instruments could not be used quickly. Therefore, a relatively simple coastal cross profile model has been set up and compared with the measurements. This costed too much time for QRF. We would recommend having a model of the study area ready beforehand in order to be able to quickly assess the effects of storms.

We recommend selecting additional QRF sites along the Dutch coast with more alongshore uniform bathymetry to set-up and validate the XBeach 1D model approach with. The beach dune system of the Dutch Holland coast would be well suited and the QRF could link up with long-term projects here (e.g. Donker et al, 2018).

Measurements

For the QRF it would be worthwhile to have bed elevation data just before and just after a storm. In combination with the measured hydrodynamics a better validation of one storm event can be done.

LiDAR measurements with a drone were due to limitations due to wind speeds (drone cannot fly above wind force 4), restrictions due to tide (beach during the day is not always dry), and limitations in accessibility (drone pilot with ferry) on Ameland not easy to carry out before and after a storm. That is why they were carried out before and after the storm season. We would recommend doing these LiDAR measurements with a helicopter that is less sensitive to wind, right after a single storm.

Placement and retrieval of pressure sensors was not possible just before and after a single storm due to constraints by tides (lowest pressure sensor at low water level and thus not always dry), and limitations in accessibility (in winter shorter daylight time) on Ameland . That is why they were placed before the storm season and picked up afterwards. We would recommend continuing this approach.

There was a lack of detailed bed level information from the shallow foreshore with sufficient resolution in space and time at Ameland NW to feed and compare the model with. We would recommend measuring this nearshore area also well before and after the storm season.

5 References

Cheung, K. F., Gerritsen, F, & Cleveringa, J. (2007). Morphodynamics and sand bypassing at Ameland Inlet, The Netherlands., Journal of Coastal Research 23(1): 106-118.

Deltares (2015). XBeach Technical Reference: Kingsday Release.

Deltares (2017). QRF Protocol - Meetlocatie Ameland Noordwest. Rapport 11200537-003-ZWS-0009. Deltares, December 2017.

Donker, J., van Maarseveen, M., Ruessink, G., 2018. Spatio-Temporal Variations in Foredune Dynamics Determined with Mobile Laser Scanning. Journal of Marine Science and Engineering 6, 126. https://doi.org/10.3390/jmse6040126

Elias, E.P.L., & Bruens, A. (2013). Beheerbibliotheek Ameland. Rapport 1207724-004-ZKS-0015. Deltares, Delft.

Hoonhout, B, & van Thiel de Vries, J.S.M. (2012).Modelling dune ero-sion, overwash and inundation of barrier islands Proceedings of theConference on Coastal Engineering: Santander.

IMARES (2014). Monitoringplan Deltaprogramma Waddengebied: Advies voor het toekomstbestendig maken van het monitoringsysteem voor waterveiligheid in het Waddengebied. Technisch Rapport C121/14.

Israël, C.G. (1998). Morfologische ontwikkeling Amelander Zeegat. Werkdocument RIKZ/OS-98.147x, Rijkswaterstaat RIKZ (Den Haag).

Israël, C.G., & Dunsbergen, D.W. (1999). Cyclic morphological development of the Ameland Inlet, proceedings of the I.A.H.R Symposium on River, Coastal and Estuarine Morphodynamics, Genova, Italy, p. 705-714.

Nederhoff, C.M, Elias, E.P.L., & Vermaas, T. (2016). Erosie op Ameland Noordwest. Modelstudie: simulaties met Delft3D en XBeach. Projectnummer: 1503-008.

Roelvink, J. A. (1993). Dissipation in random wave group incident on a beach. Coastal Engineering, 19, 127–150.

Roelvink, J. A., Reniers, A. J. H. M., van Dongeren, A. R., van Thiel de Vries, J. S. M., McCall, R. T., & Lescinski, J. (2009). Modelling storm impacts on beaches, dunes and barrier islands. Coastal Engineering, 56(11-12), 1133–1152. doi:10.1016/j.coastaleng.2009.08.006.

Sutherland, J., Peet, a. H., & Soulsby, R. L. (2004). Evaluating the performance of morphological models. Coastal Engineering, 51(8-9), 917–939. doi:10.1016/j.coastaleng.2004.07.015

Van der Spek, A. J. F., & Noorbergen H. H. S. (1992). Morphodynamica van intergetijdegebieden. Rapport Beleidscommissie Remote Sensing, Delft.

Van Rijn, L. C., Walstra, D. J. R., Grasmeijer, B., Sutherland, J., Pan, S., & Sierra, J. P.

(2003). The predictability of cross-shore bed evolution of sandy beaches at the time scale of storms and seasons using process-based profile models. Coastal Engineering, 47(3):295–327. ISSN 0378-3839.

Wesselman, D., de Winter, R., Engelstad, A., McCall, R., van Dongeren, A., Hoekstra, P., Oost, A., & van der Vegt, M. (2018). The effect of tides and storms on the sediment transport across a Dutch barrier island. Earth Surface Processes and Landforms, 43(3), 579-592.

6 Appendix

A.1 Difference measured and modelled wave height for all pressure sensors for both scenarios

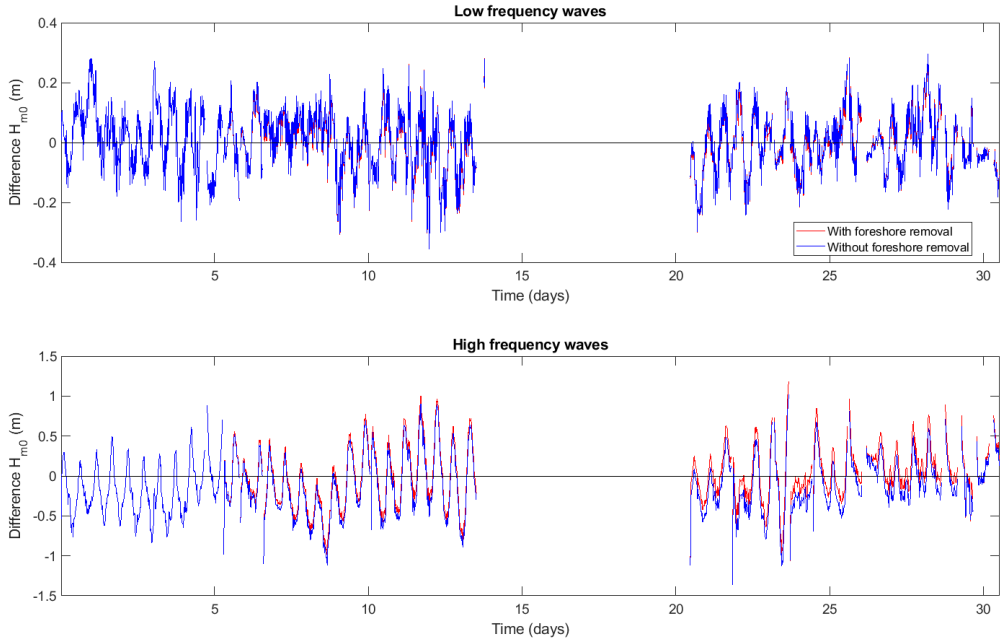

Figure A.1.Difference between measured and modelled low frequency (upper panel) and high frequency (lower panel) wave height at pressure sensors 055180 for a scenario with shoreface removal (red) and a scenario without shoreface removal (blue).

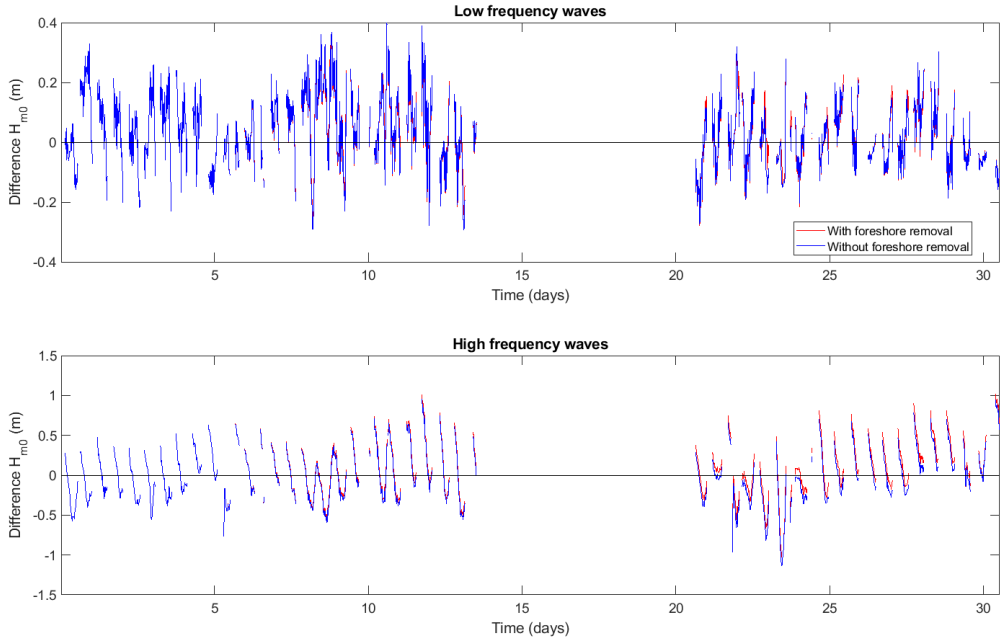

Figure A.2. Difference between measured and modelled low frequency (upper panel) and high frequency (lower panel) wave height at pressure sensors 055181 for a scenario with shoreface removal (red) and a scenario without shoreface removal (blue).

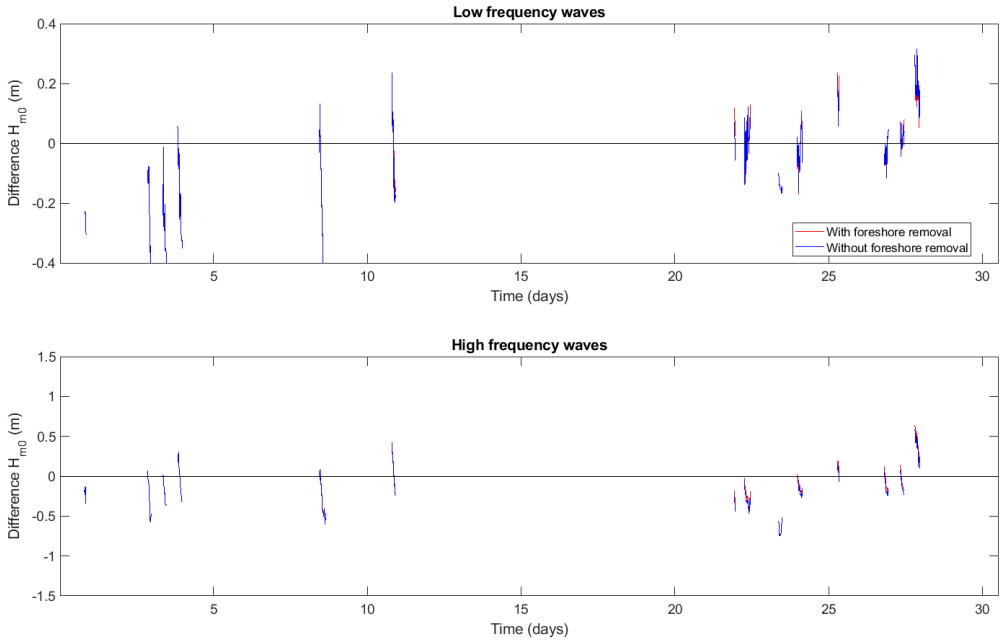

Figure A.3. Difference between measured and modelled low frequency (upper panel) and high frequency (lower panel) wave height at pressure sensors 055182 for a scenario with shoreface removal (red) and a scenario without shoreface removal (blue).